Decentralized store-and-forward based strategies for the signal control problem in large-scale congested urban road networks

Leonardo Pedroso[1] and Pedro Batista[1]

[1] *Institute for Systems and Robotics, Instituto Superior Técnico, Universidade de Lisboa, Portugal*

Accepted version[1]

Accepted on 16 Sep 2021

Cite as

L. Pedroso and P. Batista, 'Decentralized store-and-forward based strategies for the signal control problem in large-scale congested urban road networks', *Transportation Research Part C: Emerging Technologies*, vol. 132, p. 103412, 2021. doi: 10.1016/j.trc.2021.103412.

[1] Level of access, as per info available on Sherpa Romeo: `https://v2.sherpa.ac.uk/id/publication/15887` (17 Dec 2022)

Decentralized store-and-forward based strategies for the signal control problem in large-scale congested urban road networks

Leonardo Pedroso[a,*], Pedro Batista[a]

[a]*Institute for Systems and Robotics, Instituto Superior Técnico, Universidade de Lisboa, Portugal*

Abstract

Signal control strategies for congested urban road networks designed in a centralized framework require many communication links, serious processing power, and infrastructure for the centralized coordination. As a result, strategies based on a centralized framework are not scalable. The use of decentralized signal control strategies for large-scale urban traffic networks is a solution to this problem, since it allows for the implementation of such strategies on networks whose centralized solution is not easily scalable. This paper addresses the problem of designing a decentralized traffic-responsive signal control solution, proposing two methods based on different formulations of the store-and-forward model: i) the Decentralized Traffic-responsive Urban Control (DTUC) method; and ii) the Decentralized Decoupled Traffic-responsive Urban Control (D2TUC). The decentralized configuration is such that each intersection is associated with one computational unit, with limited computational power and memory, which controls the traffic signals of the incoming links. Sufficient conditions for the controllability of the considered store-and-forward models are also presented. Both methods are validated resorting to numerical simulations of the urban traffic network of Chania, Greece, for two demand scenarios, and their performance is compared with the performance of the Traffic-responsive Urban Control (TUC) centralized strategy. One of the proposed decentralized methods, D2TUC, is shown to match the performance of TUC.

Keywords: decentralized control, quadratic optimal control, traffic signal control, store-and-forward model, traffic congestion

1. Introduction

The increasing mobility demand, which oftentimes results in serious congestion of urban road networks, motivates the study of optimized signal control strategies. In fact, these strategies allow to make use of the already available traffic network infrastructure more efficiently, alleviating traffic congestion, and increasing the throughput of vehicles. Accomplishing a reduction of congestion and an efficient management of traffic

*Corresponding author.
Email address: `leonardo.pedroso@tecnico.ulisboa.pt` (Leonardo Pedroso)

networks is crucial since it allows to decrease delays, fuel consumption, and environmental pollution. In fact, it is known for decades that significant economical losses are attributed to this issue [1]. For this reason, extensive research has been carried out, from which a collection of strategies have arisen, namely SCATS [2], SCOOT [3], PRODYN [4], UTOPIA [5], and RHODES [6]. For an extensive description of strategies currently in use, see [7]. More recently, several new strategies have arisen. One particularly promising is Traffic-responsive Urban Control (TUC), presented in [8], which is based on the store-and-forward model of a traffic network, initially proposed in [9]. TUC has been extensively studied [10, 11, 12] and has been experimentally implemented in urban traffic networks in Glasgow [13], Chania [14], and Southampton [15].

However, the vast majority of signal control strategies is designed considering a centralized framework, which requires many communication links, serious processing power, and infrastructure for the centralized coordination. In fact, the implementation of a centralized configuration requires all-to-all communication, via one ou more central units. This configuration requires that there is communication between every node and a central unit, which can be achieved by a path of several physical communication links. These are the same physical links that are used in a decentralized configuration. The big difference is the amount of information that needs to be handled at the protocol level. On one hand, in a decentralized configuration, only local information is transmitted. On the other hand, in a centralized configuration, information has to be retransmitted via several nodes to the centralized unit, which receives information from all nodes. As the dimension of the network increases, the load on the communication links increases, the communication delays increase, and the complexity of the protocol increases, which makes the implementation of a centralized solution challenging for a large-scale network. Moreover, these strategies offer little robustness to failure of the central processing node or the communication infrastruture. As a result, in general, strategies based on a centralized framework are not easily scalable. Over the past decades, decentralized solutions have emerged as an alternative to the use of well known centralized solutions, whose implementation becomes more challenging and expensive as the dimension of the network increases. The popularity of distributed solutions is also increasing with the widening of its applications to a broad range of engineering fields. Examples of such applications are unmanned aircraft formation flight [16, 17], unmanned underwater formations [18, 19], satellite constellations [20], and irrigation networks [21]. Despite that, very little research has been undergone into decentralized signal control of large-scale urban road networks. In fact, the use of decentralized solutions allows for the implementation of signal control strategies to large-scale networks, in which the cost and infrastructure requirements of a centralized solution render it difficult to implement. One of the few works on decentralized signal control is [22]. It is based on the junction based scheduling problem, whose complexity increases exponentially due to the combinatorial nature of the problem. This work tackles this problem by aggregating vehicles on routes into sequences of clusters, which allows to find near optimal solutions efficiently. However, it makes limiting assumptions on the network topology, considering non-overlapping intersection routes. Other decentralized approaches have also been proposed making use of the back-pressure principle [23, 24] and reinforcement learning techniques [25]. In [26], the performance of the back-pressure [23] and junction based scheduling [22] decentralized algorithms were compared to the performance obtained with TUC, which is based on a centralized framework. It was found that only TUC and the back-pressure algorithm are able to achieve high performance under different demand scenarios, with TUC overperforming under congested traffic conditions and underperforming in less congested conditions, in relation to the back-pressure algorithm. Recently, another approach found in the literature is to decouple the traffic network into nodes, or clusters of nodes [27, 28, 29]. Applying standard control techniques to each of the nodes or clusters allows to obtain a control law that can be implemented in a decentralized configuration. However, each local minimization iteration does not take into account its effect on the local performance of the remaining nodes, thus this solution is sub-optimal. Conversely, in the novel approach proposed in this paper, the network is treated globally, as far as the synthesis of the gains is considered, subject to a constraint that arises from the decentralized configuration of the network, as seen in the sequel. The decentralized control solutions proposed in this paper are based on the classic principles of optimal control. Nevertheless, there are more techniques, which could be applied instead, such as linear matrix inequality (LMI) based methods [30, 31, 18]. It is not possible to formulate the decentralized control problem as an LMI, only as a bilinear matrix inequality, to which even finding just a feasible solution is NP-hard. However, to circumvent this problem: i) an iterative procedure may be followed [30, 18], whose iterations consist of LMIs; or ii) it is also possible to exploit the structure of a particular control problem to formulate it as an LMI [31]. Nevertheless, these methods have major drawbacks: i) the solution is sub-optimal; and ii) the iterative procedure requires significant computational power.

In this context, this paper addresses the problem of designing a decentralized traffic-responsive signal control solution for a large-scale congested urban road network. The proposed control solutions are based on the store-and-forward model of a traffic network, which allows to formulate the originally combinatorial model as a simplified continuous model. Thus, instead of the exponential complexity associated with combinatorial models, it is possible to achieve polynomial complexity with the proposed methods. Stage synchronization or cycle duration optimization are not considered, which have to be adjusted making use of an external algorithm (see [12] for more details). This paper builds on seminal state-of-the-art research, in particular the outstanding work and results presented by the TUC group [8, 10, 11, 12, 13, 14, 32]. These proved to be of the utmost importance to the development of the findings presented herein, as it will be highlighted throughout the paper. It is assumed that each intersection is associated with one computational unit, with limited computational power and memory, which controls the traffic signals of the incoming links. Also, only restricted communication between the computational units of two intersections sharing a link is allowed. In this paper, two methods are presented, each formulated as a classical linear-quadratic regulator problem on a different formulation of the store-and-forward model. For both methods, the regulator problem is formulated for the global traffic network, with a given sparsity constraint on the regulator gain.

Such sparsity constraints impose certain entries of the global gain matrix to be null, following a structure that reflects the decentralized nature of the network, necessary for the implementation of the decentralized regulator. The first method, denoted herein as Decentralized Traffic-responsive Urban Control (DTUC) method, is essentially a decentralized version of the TUC strategy. The derivation of this method also provides insight into the operation of TUC. The second method, designated herein as Decentralized Decoupled Traffic-responsive Urban Control (D2TUC), is inspired in the principle of the centralized Qudratic Programming Control (QPC) method proposed in [32] as an attempt to improve the performance obtained with TUC. Finally, both methods are validated resorting to numerical simulations of the urban traffic network of Chania, Greece, and their performance is compared with the performance obtained with TUC.

This paper is organized as follows. In Section 2, the control problem is formulated, introducing the store-and-forward model and the decentralized configuration paradigm. In Sections 3 and 4, the DTUC and D2TUC signal control methods are derived, respectively. In Section 5, both methods are validated resorting to numerical simulations of a urban traffic network, and their performance is compared with the performance obtained with TUC, a state-of-the-art centralized method. Finally, Section 6 presents the main conclusions of this paper.

1.1. Notation

Throughout this paper, the identity and null matrices, both of appropriate dimensions, are denoted by $\mathbf{I}$ and $\mathbf{0}$, respectively. Alternatively, $\mathbf{I}_n$ and $\mathbf{0}_{n\times m}$ are also used to represent the $n \times m$ identity matrix and the $n \times m$ null matrix, respectively. The vector of ones, of appropriate dimensions, is denoted by $\mathbf{1}$. Alternatively, $\mathbf{1}_n$ is used to denote the vector of ones of dimension n. The i-th component of a vector $\mathbf{v} \in \mathbb{R}^n$ is denoted by $[\mathbf{v}]_i$, and the entry (i,j) of a matrix $\mathbf{A}$ is denoted by $[\mathbf{A}]_{ij}$. The column wise concatenation of vectors $\mathbf{x_1}, \ldots, \mathbf{x_N}$ is denoted by $\mathrm{col}(\mathbf{x_1}, \ldots, \mathbf{x_N})$. The block diagonal matrix whose diagonal blocks are given by matrices $\mathbf{A_1}, ..., \mathbf{A_N}$ is denoted by $\mathrm{diag}(\mathbf{A_1}, ..., \mathbf{A_N})$. Moreover, $\mathrm{diag}(\mathbf{v}) \in \mathbb{R}^{n\times n}$, where $\mathbf{v} \in \mathbb{R}^n$ is a vector, denotes the diagonal matrix whose diagonal entries correspond to the entries of $\mathbf{v}$. Given a symmetric matrix $\mathbf{P}$, $\mathbf{P} \succ \mathbf{0}$ and $\mathbf{P} \succeq \mathbf{0}$ are used to point out that $\mathbf{P}$ is positive definite and positive semidefinite, respectively. The cardinality of a set $\mathcal{A}$ is denoted by $|\mathcal{A}|$.

2. Problem statement

The decentralized traffic-responsive control strategies proposed in this paper are based on the store-and-forward model of traffic networks. In this section, the store-and-forward model is presented for the sake of completeness. Afterwards, the decentralized signal control problem is formulated. Given that the parameters of a traffic network vary slowly with time, time-invariant parameters that characterize the traffic network are considered.

2.1. Store-and-forward model

The store-and-forward model presented herein closely follows the one presented in [8, 32]. In addition, more details on the computation of the dynamics matrices are given herein, as well as sufficient conditions for the controllability of the LTI systems that arise from this model. The topology of a traffic network, which is assumed to be time invariant, can be defined by the interconnection of the junctions via directional links. Such topology may be represented by a directed graph, or digraph, $\mathcal{G} := (\mathcal{V}_\mathcal{G}, \mathcal{E}_\mathcal{G})$, composed of a set $\mathcal{V}_\mathcal{G}$ of vertices and a set $\mathcal{E}_\mathcal{G}$ of directed edges. An edge e incident on vertices i and j, directed from j towards i, is denoted by $e = (j, i)$. For a vertex i, its in-degree, ν_i^-, is the number of edges directed towards it, and $\mathcal{E}_i^-$ is the set of such edges. Conversely, for a vertex i, its out-degree, ν_i^+, is the number of edges directed from it, and $\mathcal{E}_i^+$, is the set of such edges. A directed walk of length n is an ordered sequence of edges denoted by $p = (e_1, \ldots, e_{n-1})$ for which there exists a sequence of vertices $(v_1, \ldots, v_n)$ such that $e_i = (v_i, v_{i+1})$. For a more detailed overview of the elements of graph theory used to model this network, see [33, 34].

Consider a traffic network with links $z \in \{1, \ldots, Z, Z+1 \ldots, \tilde{Z}\}$ and signalized junctions $j \in \{1, \ldots, J\}$. In this framework, each junction is represented by a vertex, *i.e.* junction j is represented by vertex j, and if there is a directional link z from junction i towards junction j, then this link is represented by an edge directed from vertex i towards vertex j, *i.e.*, edge $e_z = (i, j)$ with $z \in \{1, ..., Z\}$. If there is a link z from outside of the network towards a vertex j then it represented by $e_z = (0, j)$, with $z \in \{1, ..., Z\}$. Conversely, a link z directed from a vertex j towards outside of the network is represented by $e_z = (j, 0)$, with $z \in \{Z+1, ..., \tilde{Z}\}$. Links $z \in \{Z+1, ..., \tilde{Z}\}$ are not considered in the traffic network control, since their flow is not controlled by any of the junctions.

According to the configuration of the network, a vehicle in link z has the possibility to turn to link $w \in O_z$, where

$$O_z := \left\{ w \in \mathbb{N} : \exists j \in \{1, \ldots, J\} : e_z \in \mathcal{E}_j^- \wedge e_w \in \mathcal{E}_j^+ \right\} \ .$$

Conversely, the set of links with the possibility of turning to link z is defined as

$$I_z := \left\{ w \in \mathbb{N} : \exists j \in \{1, \ldots, J\} : e_w \in \mathcal{E}_j^- \wedge e_z \in \mathcal{E}_j^+ \right\} \ .$$

Each link z is characterized by: i) a saturation flow $S_z \in \mathbb{R}^+$, expressed in vehicles per unit of time; ii) turning rates $t_{w,z} \in [0, 1]$, where $w \in I_z$; and iii) the link exit rate $t_{z,0} \in [0, 1[$. Define the turning rate matrix $\mathbf{T} \in \mathbb{R}^{Z \times Z}$ as

$$[\mathbf{T}]_{zw} := \begin{cases} t_{w,z} \ , & w \in I_z \\ 0 \ , & w \notin I_z \end{cases} \ , \quad z, w \in \{1, \ldots, Z\} \ ,$$

and the exit rates vector $\mathbf{t_0} := [t_{1,0} \ \ldots \ t_{Z,0}]^T \in \mathbb{R}^Z$. It is important to remark that, for two links z and w, which, respectively, arrive at and depart from a junction j, *i.e.*, $w \in O_z$, it may be the case that it is not allowed to turn from z to w. In that case, one sets $t_{z,w} = 0$. Also, if for an edge e_z, $z \in \{1, \ldots, Z\}$, there exists $e_w \in \mathcal{E}_\mathcal{G}$, $w \in \{Z+1, \tilde{Z}\}$, with $t_{z,w} \neq 0$, then the sum of the entries of the z-th column of $\mathbf{T}$ is less than or equal to one, and equal to one otherwise.

A traffic network at a given instant is defined by the triplet $(\mathcal{G}, \mathbf{T}, \mathbf{t_0})$, which may be time-varying. Note that there are possible configurations of $(\mathcal{G}, \mathbf{T}, \mathbf{t_0})$ that are not physically meaningful in the context of the problem. For that reason, one may define a subset of traffic networks of finite dimension and for which vehicles are not permanently trapped inside it, as detailed in the following definitions, without any loss of generality in the context of traffic network control. Note that a vehicle may exit the network either by entering an edge e_z which is of the form $e_z = (j, 0)$, or whose exit rate $t_{z,0}$ is non-zero.

Definition 2.1 (Open traffic network)**.** *A traffic network characterized by $(\mathcal{G}, \mathbf{T}, \mathbf{t_0})$ is said to be open if, for every edge of the network $e_z \in \mathcal{E}_\mathcal{G}$, there is a directed walk starting at e_z which a vehicle may follow to exit the network with non-zero probability.*

Definition 2.2 (Feasible traffic network)**.** *A traffic network characterized by $(\mathcal{G}, \mathbf{T}, \mathbf{t_0})$ is said to be feasible if*

1. *$\mathcal{E}_\mathcal{G}$ and $\mathcal{V}_\mathcal{G}$ are finite sets;*
2. *$(\mathcal{G}, \mathbf{T}, \mathbf{t_0})$ is open.*

The signal control strategy for each junction j is based on cycles of a given duration C_j, which for the sake of simplicity is considered to be constant and equal to C across all junctions. For each cycle of junction j, there is a fixed number of stages, which belong to the set $\mathcal{F}_j$, each defined by an unique integer $s \in \{1, \ldots, S\}$ network-wise. Each stage s has an associated green time g_s, that is the control variable, which must satisfy the constraint

$$g_s \geq g_{s,\min} \ , \quad s \in \{1, \ldots, S\} \ , \tag{1}$$

where $g_{s,\min} \in \mathbb{R}$ is the minimum permissible green time for stage s. This constraint is necessary to guarantee sufficient green time allocated to the pedestrian phases that are allowed during stage s. Then, each cycle has to satisfy the constraint

$$\sum_{s \in \mathcal{F}_j} g_s + L_j = C \ , \quad j \in \{1, \ldots, J\} \ , \tag{2}$$

where L_j is the lost time per cycle at junction j. The lost time at a junction, also designated as intergreen time, is the time of all-red signals of that junction, during a whole cycle, which is necessary to provide a temporal safety margin between the instant a stage is set to red and the instant another stage is set to green. For each stage, there is a set of links which have right of way (r.o.w.). Define the stage matrix $\mathbf{S} \in \mathbb{R}^{Z \times S}$ as

$$[\mathbf{S}]_{zs} := \begin{cases} 1 \ , & \text{if link } z \text{ has r.o.w. at stage } s \\ 0 \ , & \text{otherwise} \end{cases} \ .$$

Definition 2.3 (Minimum complete stage strategy)**.** *A stage strategy characterized by the stage matrix* $\mathbf{S}$ *is said to be a minimum complete stage strategy if*

1. *every stage gives r.o.w. to at least one link, i.e.,* $\forall s \in \{1, \ldots, S\}\ \exists z : [\mathbf{S}]_{zs} = 1$*;*
2. *each link has a stage in which it is given r.o.w., i.e.,* $\forall z \in \{1, \ldots, Z\}\ \exists s : [\mathbf{S}]_{zs} = 1$*;*
3. *stages of a given junction can only give r.o.w. to links directed towards that junction, i.e.,* $\forall j \in \{1, \ldots, J\}\ \forall s \in \mathcal{F}_j\ \forall z \in \{1, \ldots, Z\}\ [\mathbf{S}]_{zs} = 1 \implies e_z \in \mathcal{E}_j^-$*;*
4. *the set of links that are given r.o.w. for each stage in a junction is linearly independent, i.e.,* $\forall j \in \{1, \ldots, J\}\ \forall s_1, s_2 \in \mathcal{F}_j\ s_1 \neq s_2 \implies \nexists k \in \mathbb{R} : [\mathbf{S}]_{s_1} = k[\mathbf{S}]_{s_2}$*, where* $[\mathbf{S}]_s$ *denotes the s-th column of* $\mathbf{S}$.

Without loss of generality, the following numbering convention is used to ease the notation throughout this paper, following the procedure: i) a natural number is attributed to each junction with no particular criterion; ii) a natural number is attributed to each link, starting by those incident on junction 1, *i.e.*, edges in $\mathcal{E}_1^-$, followed by edges in $\mathcal{E}_2^-$ and so forth until the edges in $\mathcal{E}_J^-$ are numbered; iii) natural numbers are then attributed to the remaining edges, which are of the form $e_z = (j, 0)$, with no particular criterion; iv) natural numbers are attributed to each stage, whose purpose is detailed in the sequel, starting by those which give r.o.w. to links in $\mathcal{E}_1^-$, followed by those which give r.o.w to links in $\mathcal{E}_2^-$, and so forth.

Consider now a link z and denote the number of vehicles in link z as $x_z(k)$ at time kC, where k is the discrete time instant and the cycle time C is the chosen sampling time. The dynamics are modeled by the vehicle conservation equation

$$x_z(k+1) = x_z(k) + C\left(q_z(k) - u_z(k) + d_z(k) - s_z(k)\right)\ , \tag{3}$$

where $u_z(k)$ is the outflow of link z; $q_z(k)$ is the inflow given by

$$q_z(k) = \sum_{w \in I_z} t_{wz} u_w(k)\ ; \tag{4}$$

$d_z(k)$ is the demand within the link; and $s_z(k)$ is the exit flow within the link, set to $s_z(k) = t_{z,0} q_z(k)$. Additionally, links are subject to constraints

$$0 \leq x_z(k) \leq x_{z,\max}\ , \quad z \in Z\ , \tag{5}$$

where $x_{z,\max} \in \mathbb{R}$ denotes the maximum admissible number of vehicles in link z. To satisfy this constraint, an upstream gating may be put in place in order to avoid overloading any links during periods of high demand. More details on this nonlinear imposition are given in Section 2.2, and its effects are exemplified and discussed in Section 5.

After some algebraic manipulations, detailed in Appendix A, it is possible to write the dynamics as an LTI system with a time-varying disturbance

$$\mathbf{x}(k+1) = \mathbf{A}\mathbf{x}(k) + \mathbf{B_u}\mathbf{u}(k) + C\mathbf{d}(k)\ , \tag{6}$$

where $\mathbf{x}(k) := \mathrm{col}(x_1(k), ..., x_Z(k)) \in \mathbb{R}^Z$, $\mathbf{u}(k) := \mathrm{col}(u_1(k), ..., u_Z(k)) \in \mathbb{R}^Z$, $\mathbf{d}(k) := \mathrm{col}(d_1(k), ..., d_Z(k)) \in \mathbb{R}^Z$, $\mathbf{A} = \mathbf{I}_Z$, and

$$\mathbf{B_u} = C\left(\left(\mathbf{I}_Z - \mathrm{diag}(\mathbf{t_0})\right)\mathbf{T} - \mathbf{I}_Z\right) . \tag{7}$$

However, note that the components of $\mathbf{u}(k)$ in (6) cannot be independently selected, as they depend on the different admissible stages at each junction. Nevertheless, (6) is of great interest as far as the simulation of the network is concerned, due to the ease to include nonlinear constraints such as (5), as put forward in Section 2.2. As a matter of fact, in Section 5, it is the basis for the nonlinear numeric simulation of a traffic network as a means of assessing the performance of the control strategies proposed herein.

The store-and-forward model is mainly characterized by the following simplification of the traffic flow, which models green-red switchings within a whole cycle as a continuous flow of vehicles. Consider a link z, and conditions in which constraint (5) is satisfied, *i.e.* there is room to store vehicles in every link $w \in O_z$, and in which $x_z(k)$ is large enough to allow for the maintenance of the flow of vehicles during the green time of the link. The real flow is approximately equal to the saturation flow S_z during the green time of the stages for which link z has r.o.w. and null otherwise, during each cycle. Under the store-and-forward formulation, the flow of each link is assumed to be constant and equal to its average value, during a whole cycle. Thus, the control sampling time is set to the cycle time C and the modeled flow is given by

$$u_z(k) = S_z \frac{G_z(k)}{C} \; , \quad z \in \{1, \ldots, Z\} \; , \tag{8}$$

where k is the discrete time instant, and $G_z(k)$ is the total green time of link z, given by the summation of the green times of each stage for which link z has r.o.w., *i.e.*,

$$G_z(k) = \sum_{s:[\mathbf{S}]_{zs} \neq 0} g_s(k) \; . \tag{9}$$

Substituting (8) in (6), according to the store-and-forward model, one obtains the following LTI system with a time-varying disturbance

$$\mathbf{x}(k+1) = \mathbf{A}\mathbf{x}(k) + \mathbf{B_G}\mathbf{G}(k) + C\mathbf{d}(k) \; , \tag{10}$$

where $\mathbf{G}(k) := \mathrm{col}(G_1(k), ..., G_Z(k)) \in \mathbb{R}^Z$ and

$$\mathbf{B_G} = \frac{1}{C}\mathbf{B}_u \mathrm{diag}(S_1, \ldots, S_Z) = \left(\left(\mathbf{I}_Z - \mathrm{diag}(\mathbf{t_0})\right)\mathbf{T} - \mathbf{I}_Z\right)\mathrm{diag}(S_1, \ldots, S_Z) \in \mathbb{R}^{Z \times Z} \; . \tag{11}$$

Similarly to (6), the components of the command action in (10), $\mathbf{G}(k)$, cannot be independently selected, since they depend on the different admissible stages at each junction. However, the D2TUC control strategy, proposed in Section 4, makes use of this LTI system to find a suitable command action $\mathbf{G}(k)$, as if it were possible to optimize its components independently, and then apply a post-processing algorithm, as detailed in the sequel, to allocate the green times among the stages.

Substituting (9) in (6) and still considering the sampling time to be equal to the cycle time, according to the store-and-forward model, after some algebraic manipulation, as detailed in Appendix A, one obtains the LTI system with a time-varying disturbance

$$\mathbf{x}(k+1) = \mathbf{A}\mathbf{x}(k) + \mathbf{B_g}\mathbf{g}(k) + C\mathbf{d}(k) \;, \tag{12}$$

where $\mathbf{g}(k) := \text{col}(g_1(k), ..., g_S(k)) \in \mathbb{R}^S$ and

$$\mathbf{B_g} = \mathbf{B_G}\mathbf{S} = \left(\left(\mathbf{I}_Z - \text{diag}(\mathbf{t_0})\right)\mathbf{T} - \mathbf{I}_Z\right)\text{diag}(S_1, \ldots, S_Z)\mathbf{S} \in \mathbb{R}^{Z\times S} \;. \tag{13}$$

The components of the command action in (12), $\mathbf{g}(k)$, are the green times of each stage, thus can be independently selected. The DTUC control strategy, proposed in Section 3, makes use of this LTI system to find a suitable command action $\mathbf{g}(k)$.

It is assumed that one can sense the full state $\mathbf{x}(k)$. Thus, the output of the discrete-time systems (10) and (12), with sampling time equal to the cycle time C are given by

$$\mathbf{y}(k) = \mathbf{C}\mathbf{x}(k) \;, \tag{14}$$

where $\mathbf{y}(k) := \text{col}(y_1(k), ..., y_Z(k)) \in \mathbb{R}^Z$ is the output and $\mathbf{C} = \mathbf{I}_Z$. For practical applications, the state has to be estimated with an observer that relies on sensing devices. For a detailed overview of vehicle detection sensor networks, see [35], and for a recent low-cost approach, see [36]. However, in a decentralized control application, limited information is available. Thus, $\mathbf{y}(k)$ is not available to any junction in its whole, as discussed in Section 2.4.

The store-and-forward model of a traffic network models the average flow of vehicles instead of considering the real interrupting flow. This formulation allows to approximate a combinatorial model with an LTI model of the traffic network, whose control law synthesis techniques are not only well studied, but also efficient. However, given that it is not sensible to green-red stage switching, it is not sensible to either stage synchronization or cycle duration, which have to be adjusted making use of an external algorithm. An example of such an algorithm was developed for TUC in [12]. Moreover, this simplification is valid only under conditions in which constraint (5) is satisfied, which is often not the case for high demand scenarios. For this reason, additional nonlinear post-processing of the green times, computed for the store-and-forward model, is required. As a result, this simplification evidently leads to a sub-optimal solution of the original combinatorial control problem.

2.2. Nonlinear model

Although it is very convenient to work with a linear model for controller synthesis purposes, such as the store-and-forward model, it is insufficient to simulate the network dynamics and assess the performance of a control law, since the nonlinear constraint (5) is not enforced. For that reason, a nonlinear model is introduced, as a means of assessing the performance of the store-and-forward based control laws. As put forward in [32], adapting the store-and-forward model, a simple nonlinear discrete-time model can be employed. Considering a sampling time $T \ll C$ and assuming, for simplicity, that $C/T \in \mathbb{N}$, it is possible to write

$$\begin{cases} \mathbf{x}(k_T+1) = \mathbf{A}\mathbf{x}(k_T) + \frac{T}{C}\mathbf{B_u}\mathbf{u_{nl}}(k_T) + T\mathbf{d}(k_T) \\ \mathbf{y}(k_T+1) = \mathbf{C}\mathbf{x}(k_T) \end{cases}, \tag{15}$$

as put forward in [32], where k_T is the discrete time instant corresponding to time $k_T T$ and $\mathbf{u_{nl}}(k_T) := \mathrm{col}(u_{nl,1}(k_T), ..., u_{nl,Z}(k_T)) \in \mathbb{R}^Z$ with

$$u_{nl,z}(k_T) = \begin{cases} 0\,, & \exists w \in O_z : t_{z,w} \neq 0 \wedge x_w(k_T) > c_{ug}x_{w,\max} \\ \min\{x_z(k_T)/T, u_z(k = \lfloor K_T T/C \rfloor)\}\,, & \text{otherwise} \end{cases},$$

as put forward in [32], in which $u_z(k)$ is the command action, which is updated every cycle C, whose synthesis is based on a linear model as defined in (8), and $c_{ug} \in]0,1[$ is a parameter to be tuned in order to adjust the sensitivity of upstream gating. Note that, in this model, constraint (5) is modeled.

2.3. Illustrative traffic network

Consider an illustrative section of an urban road, as depicted in Fig. 1, containing a roundabout with three signalized entries out of a total of four entries, and an intersection. Fig. 2 depicts the traffic network topology graph, whereas the associated stage organization is presented in Table 1, with $J = 5$ junctions, $Z = 11$ links, and $S = 9$ stages. The exit rate and saturation flow of each link of the illustrative traffic network is shown in Table 2. The numbering convention proposed in Section 2.1 was used.

Table 1: Stage organization of the illustrative traffic network.

Junction j	1		2		3	4		5	
Stages	1	2	3	4	5	6	7	8	9
Links with r.o.w.	$\{1\}$	$\{2\}$	$\{3\}$	$\{4\}$	$\{5,6\}$	$\{7\}$	$\{8\}$	$\{9,11\}$	$\{10\}$

Table 2: Exit rate and saturation flow of each link of the illustrative traffic network.

Link z	1	2	3	4	5	6	7	8	9	10	11
$t_{z,0}$	0.05	0	0.04	0	0.1	0	0.02	0	0.05	0.03	0.01
$S_z(\mathrm{veh\,min}^{-1})$	50	50	50	50	35	50	50	50	55	10	60

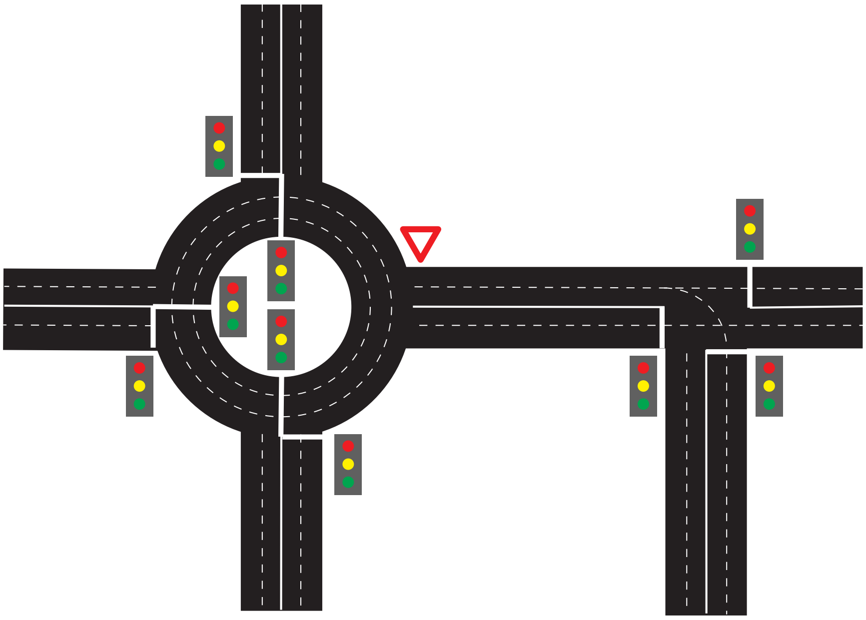

Figure 1: Illustrative traffic network.

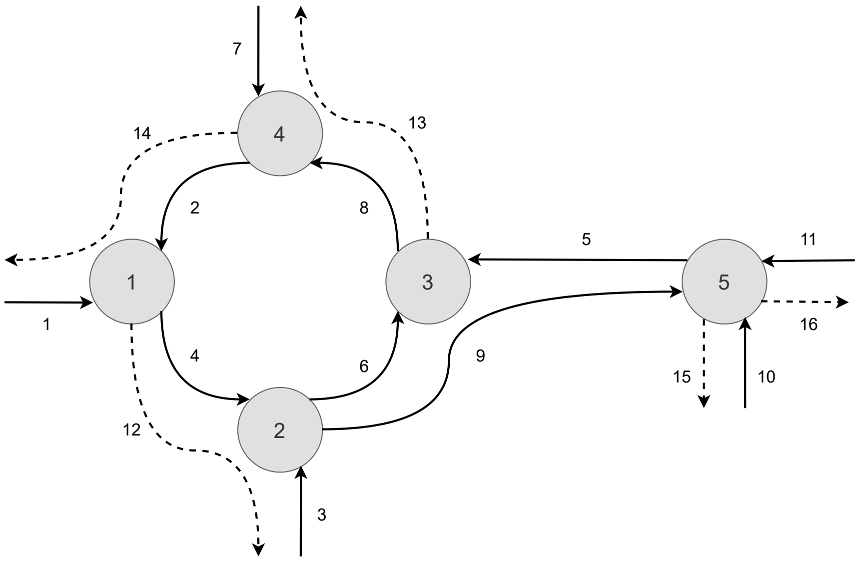

Figure 2: Illustrative traffic network topology graph.

According to the definitions above, it follows that the stage matrix **S** and a possible turning rate matrix

$\mathbf{T}$ are given by

$$\mathbf{S} = \begin{bmatrix} 1 & 0 & 0 & 0 & 0 & 0 & 0 & 0 & 0 \\ 0 & 1 & 0 & 0 & 0 & 0 & 0 & 0 & 0 \\ 0 & 0 & 1 & 0 & 0 & 0 & 0 & 0 & 0 \\ 0 & 0 & 0 & 1 & 0 & 0 & 0 & 0 & 0 \\ 0 & 0 & 0 & 0 & 1 & 0 & 0 & 0 & 0 \\ 0 & 0 & 0 & 0 & 1 & 0 & 0 & 0 & 0 \\ 0 & 0 & 0 & 0 & 0 & 1 & 0 & 0 & 0 \\ 0 & 0 & 0 & 0 & 0 & 0 & 1 & 0 & 0 \\ 0 & 0 & 0 & 0 & 0 & 0 & 0 & 1 & 0 \\ 0 & 0 & 0 & 0 & 0 & 0 & 0 & 0 & 1 \\ 0 & 0 & 0 & 0 & 0 & 0 & 0 & 1 & 0 \end{bmatrix} \text{ and } \mathbf{T} = \begin{bmatrix} 0 & 0 & 0 & 0 & 0 & 0 & 0 & 0 & 0 & 0 & 0 \\ 0 & 0 & 0 & 0 & 0 & 0 & 0.3 & 0.4 & 0 & 0 & 0 \\ 0 & 0 & 0 & 0 & 0 & 0 & 0 & 0 & 0 & 0 & 0 \\ 0.6 & 0.4 & 0 & 0 & 0 & 0 & 0 & 0 & 0 & 0 & 0 \\ 0 & 0 & 0 & 0 & 0 & 0 & 0 & 0 & 0 & 0.6 & 0.9 \\ 0 & 0 & 0.7 & 0.5 & 0 & 0 & 0 & 0 & 0 & 0 & 0 \\ 0 & 0 & 0.3 & 0 & 0 & 0 & 0 & 0 & 0 & 0 & 0 \\ 0 & 0 & 0 & 0 & 0.8 & 1 & 0 & 0 & 0 & 0 & 0 \\ 0 & 0 & 0 & 0.5 & 0 & 0 & 0 & 0 & 0 & 0 & 0 \\ 0 & 0 & 0 & 0 & 0 & 0 & 0 & 0 & 0 & 0 & 0 \\ 0 & 0 & 0 & 0 & 0 & 0 & 0 & 0 & 0 & 0 & 0 \end{bmatrix},$$

respectively. It is important to remark that this network is feasible and the illustrative stage strategy is minimum complete, according to the aforementioned definitions. Note that, in junctions j where there may be a flow of vehicles exiting the network under study via a link $e_z = (j, 0)$, represented in Fig. 2 by dashed links, the summation of the j-th column of $\mathbf{T}$ does not amount to one. It is also important to remark that, although there is no signaling in junction 3, a vertex with a single stage was added with the purpose of dividing the queue on link 8 into traffic coming from the roundabout and link 5. In this way, the constraint (2) with $L_5 = 0$ ensures that traffic from links 5 and 6 is always allowed, unless there is no room for vehicles in link 8, which is monitored by constraint (5), which is taken into account in the nonlinear model presented in Section 2.2. The fact that vehicles coming from link 6 to 8 have r.o.w. over those coming from 5 to 8 is modeled by the difference in their average saturation flows S_6 and S_5. Note that both links are given an artificial green time in the model, and they have a similar throughput capacity without considering the priority of the vehicles. Nevertheless, link 5 has a significantly lower saturation flow, because all vehicles coming from link 5 ought to yield if there is traffic coming from 6, which reduces the macroscopic throughput of vehicles in link 5.

2.4. Decentralized configuration

Assume that each junction j is associated with one computational unit $\mathcal{T}_j$, with limited computational power and memory, which controls the traffic signals. Moreover, communication between $\mathcal{T}_j$ and $\mathcal{T}_i$ is allowed if there is a link between junctions j and i with either direction. This communication link is usually necessary for the integration of an observer based on multiple vehicle detectors. Although this problem falls out of the scope of this paper, the necessity of such links should not be disregarded. For this reason, the communication graph is similar to the network topology graph, except that all directional links of $\mathcal{G}$ are now bidirectional and each vertex now represents the corresponding computational units. Two decentralized configurations are considered: i) configuration Ψ, for which each computational unit $\mathcal{T}_j$ has access only to the queue length of the links arriving or departing from junction j, *i.e.*, $x_z(k),\ e_z \in \Psi_j$, where

$$\Psi_j = \mathcal{E}_j^- \cup \mathcal{E}_j^+ \; ; \tag{16}$$

and ii) configuration Φ, for which each computational unit $\mathcal{T}_j$ has access to the queue length of not only the links arriving and departing from junction j but also of all the links arriving at and departing from every junction with which $\mathcal{T}_j$ has a communication link, which are, as aforementioned, all junctions with at least a link connected to junction j with either direction, *i.e.*, $x_z(k),\ e_z \in \Phi_j$, where

$$\Phi_j = \bigcup_{i\in\phi_j} (\mathcal{E}_i^- \cup \mathcal{E}_i^+) \quad \text{and} \quad \phi_j = \left\{ i \in \{1,\ldots,J\} : (\mathcal{E}_j^- \cap \mathcal{E}_i^+) \cup (\mathcal{E}_j^+ \cap \mathcal{E}_i^-) \neq \varnothing \right\} \; . \tag{17}$$

Note that $\Psi_j \subseteq \Phi_j$. In fact, for the decentralized configuration Ψ, no queue length information is transmitted via the established communication links, required by a decentralized observer. In other words, in this configuration, the controller of a given junction does not require information that is not already available to allow for the operation of a decentralized state observer. In configuration Φ, the information known to each of the junctions is shared via the established communication links. In the sequel, the difference of performance between these configurations is assessed, with particular emphasis to whether or not the increase in communication load originates an appreciable improvement of the traffic control performance.

The control problem at hand is, then, to find a steady-state control technique that relies on state feedback and follows the following guidelines:

1. The computational load of the control algorithm of the network must be distributed across all computational units in a way such that each caries out computations concerning their own signaling command action exclusively, which circumvents the curse of dimensionality;
2. The controller synthesis must be able to be carried out offline, as a means of avoiding intensive real-time computational loads;
3. The quantity of information exchanged in a communication link should be reduced to a minimum, and must concern the junction broadcasting the data exclusively.

3. Decentralized Traffic-responsive Urban Control (DTUC)

The first control strategy presented herein is based on the traffic dynamics model (12) and output (14). It is a decentralized version of the TUC strategy, as presented in [11, Section 3.], which is a state-of-the-art centralized solution. The derivation of this method is very distinct to the one presented in [11, Section 3] and it provides additional insight into the working principle of TUC. Consider the following result.

Proposition 3.1. Consider a feasible traffic network characterized by $(\mathcal{G}, \mathbf{T}, \mathbf{t_0})$ and a minimum complete stage strategy characterized by stage matrix $\mathbf{S}$. Let $\boldsymbol{\mathcal{C}}$ be the controllability matrix of the store-and-forward LTI system (12). Then, $\text{rank}(\boldsymbol{\mathcal{C}}) = S \leq Z$.

Proof. See Appendix B. □

Note that the LTI system (12) is the same formulation of the store-and-forward model that was used to develop TUC [11]. It follows directly from Proposition 3.1 that the store-and-forward LTI system (12) is controllable if and only if $S = Z$. Given that, in general, the number of stages S is lower than the number of links Z, *i.e.*, $S < Z$, it follows that, in general, (12) is not controllable. The following analysis is conducted to overcome the uncontrollability of the general case $S < Z$. Although it is unnecessary if $S = Z$, it remains valid for this case and all the results obtained are, at any point, easily particularized for $S = Z$. Let $\boldsymbol{\mathcal{C}}$ be the controllability matrix of the store-and-forward LTI system (12). As a means of devising a state feedback control strategy, one may decompose system (12) according to the Canonical Structure Theorem [37, Chap. 18]. For that purpose, consider a change of state variables

$$\mathbf{z}(k) = \mathbf{W}^{-1}\mathbf{x}(k) \;, \tag{18}$$

where $\mathbf{W} \in \mathbb{R}^{Z\times Z}$. In addition, the columns of $\mathbf{W}$, denoted by $\mathbf{w_1}, \dots, \mathbf{w_Z}$, are selected such that $\mathbf{w_1}, \dots, \mathbf{w_S}$ is a basis of $\text{Im}(\boldsymbol{\mathcal{C}})$ and the remaining columns $\mathbf{w_{S+1}}, \dots, \mathbf{w_Z}$ are selected such that $\mathbf{w_1}, \dots, \mathbf{w_Z}$ is a basis of $\mathbb{R}^Z$. By the Canonical Structure Theorem, the transformation of system (12), according to (18), can be decomposed into

$$\begin{bmatrix} \mathbf{z_1}(k+1) \\ \mathbf{z_2}(k+1) \end{bmatrix} = \hat{\mathbf{A}} \begin{bmatrix} \mathbf{z_1}(k) \\ \mathbf{z_2}(k) \end{bmatrix} + \hat{\mathbf{B}}_\mathbf{g}\mathbf{g}(k) + C \begin{bmatrix} \hat{\mathbf{d}}_\mathbf{1}(k) \\ \hat{\mathbf{d}}_\mathbf{2}(k) \end{bmatrix} ,$$

where $\mathbf{z_1}(k) \in \mathbb{R}^S$ is the controllable component of the state, $\mathbf{z_2}(k) \in \mathbb{R}^{Z-S}$ is the uncontrollable component of the state, and

$$\hat{\mathbf{A}} = \begin{bmatrix} \hat{\mathbf{A}}_\mathbf{11} & \hat{\mathbf{A}}_\mathbf{12} \\ \mathbf{0}_{(Z-S)\times S} & \hat{\mathbf{A}}_\mathbf{22} \end{bmatrix} = \mathbf{W}^{-1}\mathbf{A}\mathbf{W} = \mathbf{I}_Z \;,\;\; \hat{\mathbf{B}}_\mathbf{g} = \mathbf{W}^{-1}\mathbf{B}_\mathbf{g} = \begin{bmatrix} \hat{\mathbf{B}}_\mathbf{g1} \\ \mathbf{0} \end{bmatrix} \;\text{ and }\; \begin{bmatrix} \hat{\mathbf{d}}_\mathbf{1}(k) \\ \hat{\mathbf{d}}_\mathbf{2}(k) \end{bmatrix} = \mathbf{W}^{-1}\mathbf{d}(k) \;, \tag{19}$$

with $\hat{\mathbf{B}}_\mathbf{g1} \in \mathbb{R}^{S\times S}$. Writing each of the components separately yields

$$\mathbf{z_1}(k+1) = \mathbf{z_1}(k) + \hat{\mathbf{B}}_\mathbf{g1}\mathbf{g}(k) + C\hat{\mathbf{d}}_\mathbf{1}(k) \tag{20}$$

and

$$\mathbf{z_2}(k+1) = \mathbf{z_2}(k) + C\hat{\mathbf{d}}_\mathbf{2}(k) \;. \tag{21}$$

Furthermore, given that the uncontrollable component, whose dynamics are given by (21), is not stable, then, by [37, Theorem 18.28], the system (12) is not stabilizable. In fact, no matter the chosen linear feedback control law, there are $Z - S$ poles at the intersection of the unitary circumference with the positive real axis of the complex plane, *i.e.*, $Z-S$ integrator poles. It follows, by the definition of stabilizability, that there is no control law, either centralized or decentralized, of the form

$$\mathbf{g}(k) = -\mathbf{K}\mathbf{x}(k) , \tag{22}$$

where $\mathbf{K} \in \mathbb{R}^{S\times Z}$ is the feedback gain, that stabilizes (12) in closed-loop.

The analysis of the controllability of (12), making use of the Canonical Structure Theorem, seems discouraging at first sight. In fact, after closer inspection of the uncontrollable component, described by (21), one readily notes that it easily grows unbounded. However, the validity conditions of the store-and-forward model, namely the queue length constraint (5), guarantees that, in the nonlinear case, $\mathbf{z_2}(k)$ is, in fact, bounded. Also, apart from nonlinear considerations, nothing can be done to affect the uncontrollable component. Thus, one can aim to synthesize a linear state feedback control law of the form (22), as a means of driving the controllable component to zero. Note also that, in the TUC derivation in [11] the underlying nominal system dynamics and cost functional are the same as the ones considered here. The difference lies, at the synthesis level, on the fact that, herein, sparsity constraints are considered in order to account for the decentralized configuration. The approach detailed herein provides, for this reason, further insight into the underlying principle of TUC. First, one assumes that an historical demand $\mathbf{d}_{\text{hist}}(k)$ is available. Note that (20) can be rewritten as

$$\mathbf{z_1}(k+1) = \mathbf{z_1}(k) + \hat{\mathbf{B}}_{\mathbf{g1}}(\mathbf{g}(k) - \bar{\mathbf{g}}(k)) + C\hat{\boldsymbol{\epsilon}}(k) , \tag{23}$$

where $\hat{\boldsymbol{\epsilon}}(k)$ is considered to be a disturbance, given by $\hat{\boldsymbol{\epsilon}}(k) := [\mathbf{I}_S \;\; \mathbf{0}_{S\times(Z-S)}]\mathbf{W}^{-1}\mathbf{d}_{\text{hist}}(k) + \hat{\mathbf{B}}_{\mathbf{g1}}\bar{\mathbf{g}}(k)$. In order to apply a decentralized regulator to (23), $\bar{\mathbf{g}}(k)$ is selected such that the disturbance $\hat{\boldsymbol{\epsilon}}(k)$ is minimal, *i.e.*, $\bar{\mathbf{g}}(k)$ is given by the solution to

$$\underset{\bar{\mathbf{g}}(k)\in\mathbb{R}^S}{\text{minimize}} \quad \|\hat{\boldsymbol{\epsilon}}(k)\|^2 \qquad ,$$

for $k \in \mathbb{N}_0$. The optimization problem above is a least squares optimization problem, whose solution is

$$\begin{aligned}\bar{\mathbf{g}}(k) &= -\left(\hat{\mathbf{B}}_{\mathbf{g1}}^T\hat{\mathbf{B}}_{\mathbf{g1}}\right)^{-1}\hat{\mathbf{B}}_{\mathbf{g1}}^T\,[\mathbf{I}_S \quad \mathbf{0}_{S\times(Z-S)}]\mathbf{W}^{-1}\mathbf{d}_{\text{hist}}(k)\\ &= -\left(\mathbf{B_g}^T\mathbf{W}^{-T}\begin{bmatrix}\mathbf{I}_S & \mathbf{0}\\ \mathbf{0} & \mathbf{0}\end{bmatrix}\mathbf{W}^{-1}\mathbf{B_g}\right)^{-1}\mathbf{B_g}^T\mathbf{W}^{-T}\begin{bmatrix}\mathbf{I}_S & \mathbf{0}\\ \mathbf{0} & \mathbf{0}\end{bmatrix}\mathbf{W}^{-1}\mathbf{d}_{\text{hist}}(k) ,\end{aligned} \tag{24}$$

if $\hat{\mathbf{B}}_{\mathbf{g1}} \in \mathbb{R}^{S\times S}$ is full rank. Note that, by the Canonical Structure Theorem, (20) is controllable. Then, by definition, the controllability matrix of (20), denoted as $\boldsymbol{\mathcal{C}}_1 \in \mathbb{R}^{S\times S^2}$, is full rank. Moreover,

$$S = \text{rank}(\boldsymbol{\mathcal{C}}_1) = \text{rank}([\hat{\mathbf{B}}_{\mathbf{g1}} \quad \mathbf{I}_S\hat{\mathbf{B}}_{\mathbf{g1}} \quad \ldots \quad \mathbf{I}_S^{S-1}\hat{\mathbf{B}}_{\mathbf{g1}}]) = \text{rank}(\hat{\mathbf{B}}_{\mathbf{g1}}) ,$$

thus, $\hat{\mathbf{B}}_{\mathbf{g1}}$ is, in fact, necessarily full rank.

A decentralized regulator can be applied to (23), as a means of minimizing the quadratic infinite horizon cost function

$$J_\infty(k) := \sum_{\tau=k}^{\infty} \mathbf{z_1}(\tau)^T \mathbf{Q_1} \mathbf{z_1}(\tau) + (\mathbf{g}(\tau) - \bar{\mathbf{g}}(\tau))^T \mathbf{R} (\mathbf{g}(\tau) - \bar{\mathbf{g}}(\tau)) \,, \tag{25}$$

using a state feedback control law of the form (22), where $\mathbf{Q_1} \succeq \mathbf{0}$ and $\mathbf{R} \succ \mathbf{0}$ are selected matrices of appropriate dimensions. Rewriting (25) as

$$\begin{aligned} J_\infty(k) &= \sum_{\tau=k}^{\infty} \mathbf{x}(\tau)^T \mathbf{W}^{-T} \begin{bmatrix} \mathbf{Q_1} & \mathbf{0}_{S\times(Z-S)} \\ \mathbf{0}_{(Z-S)\times S} & \mathbf{0}_{(Z-S)\times(Z-S)} \end{bmatrix} \mathbf{W}^{-1}\mathbf{x}(\tau) + (\mathbf{g}(\tau) - \bar{\mathbf{g}}(\tau))^T \mathbf{R} (\mathbf{g}(\tau) - \bar{\mathbf{g}}(\tau)) \\ &= \sum_{\tau=k}^{\infty} \mathbf{x}(\tau)^T \mathbf{Q} \mathbf{x}(\tau) + (\mathbf{g}(\tau) - \bar{\mathbf{g}}(\tau))^T \mathbf{R} (\mathbf{g}(\tau) - \bar{\mathbf{g}}(\tau)) \,, \end{aligned} \tag{26}$$

where

$$\mathbf{Q} = \mathbf{W}^{-T} \begin{bmatrix} \mathbf{Q_1} & \mathbf{0}_{S\times(Z-S)} \\ \mathbf{0}_{(Z-S)\times r} & \mathbf{0}_{(Z-S)\times(Z-S)} \end{bmatrix} \mathbf{W}^{-1} \quad \text{and} \quad \begin{bmatrix} \mathbf{Q_1} & \mathbf{0}_{S\times(Z-S)} \\ \mathbf{0}_{(Z-S)\times S} & \mathbf{0}_{(Z-S)\times(Z-S)} \end{bmatrix} = \mathbf{W}^T \mathbf{Q} \mathbf{W} \,, \tag{27}$$

one concludes that (25) is equivalent to a quadratic regulation cost of the original system (12), where $\mathbf{Q}$, of appropriate dimensions, is guaranteed to be positive semidefinite, *i.e.*, $\mathbf{Q} \succeq \mathbf{0}$. Ideally, $\mathbf{Q}$ should be set to $\mathrm{diag}(1/x_{1,\max}, \ldots, 1/x_{Z,\max})$ in order to minimize the relative occupancy of each link, as suggested, for instance, in [32]. However, the structural constraint on $\mathbf{Q}$, portrayed in (27), must be obeyed. Having that in mind, one should choose $\mathbf{Q_1}$ corresponding to the ideal $\mathbf{Q}$. That is,

$$\mathbf{Q_1} = \begin{bmatrix} \mathbf{I}_S & \mathbf{0}_{S\times(Z-S)} \end{bmatrix} \mathbf{W}^T \mathrm{diag}(1/x_{1,\max}, \ldots, 1/x_{Z,\max}) \mathbf{W} \begin{bmatrix} \mathbf{I}_S \\ \mathbf{0}_{(Z-S)\times S} \end{bmatrix} \,,$$

which is equivalent, from (27), to

$$\mathbf{Q} = \mathbf{W}^{-T} \begin{bmatrix} \mathbf{I}_S & \mathbf{0} \\ \mathbf{0} & \mathbf{0} \end{bmatrix} \mathbf{W}^T \mathrm{diag}(1/x_{1,\max}, \ldots, 1/x_{Z,\max}) \mathbf{W} \begin{bmatrix} \mathbf{I}_S & \mathbf{0} \\ \mathbf{0} & \mathbf{0} \end{bmatrix} \mathbf{W}^{-1} \,.$$

Furthermore, note that, due to the limitation of the communication links between junctions in a decentralized configuration, as put forward in Section 2.4, there are constraints on the structure of the feedback gain $\mathbf{K}$. Consider a junction j. The command action of a stage $s \in \mathcal{F}_j$ is computed making use of information available to the computational unit $\mathcal{T}_j$, exclusively. The set of links whose queue length is available to the computational unit $\mathcal{T}_j$ is: i) Ψ_j, as defined in (16), for configuration Ψ; or ii) Φ_j, as defined in (17), for configuration Φ. Thus, for configuration Ψ, $g_s(k)$ is of the form

$$g_s(k) = [\bar{\mathbf{g}}(k)]_s - \sum_{e_i \in \Psi_j} [K]_{si} x_i(k) \,,$$

and, for configuration Φ, $g_s(k)$ is of the form

$$g_s(k) = [\bar{\mathbf{g}}(k)]_s - \sum_{e_i \in \Phi_j} [K]_{si} x_i(k) \,.$$

As a matter of fact, it is equivalent to imposing a sparsity constraint $\mathbf{K} \in \text{Sparse}(\mathbf{E_\Psi})$, where $\mathbf{E_\Psi} \in \mathbb{R}^{S \times Z}$ is such that

$$\forall j \in \{1, \ldots, J\}\ \forall s \in \mathcal{F}_j\ \forall w \in \{1, \ldots, Z\}\ \ (e_w \in \Psi_j \implies [\mathbf{E_\Psi}]_{sw} \neq 0) \wedge (e_w \notin \Psi_j \implies [\mathbf{E_\Psi}]_{sw} = 0)\ , \quad (28)$$

for the decentralized configuration Ψ, and $\mathbf{K} \in \text{Sparse}(\mathbf{E_\Phi})$, where $\mathbf{E_\Phi} \in \mathbb{R}^{S \times Z}$ is defined in the same manner as (28), replacing Ψ_j with Φ_j, for the decentralized configuration Φ.

Thus, the linear quadratic optimization problem becomes

$$\begin{aligned} \underset{\mathbf{K} \in \mathbb{R}^{S \times Z}}{\text{minimize}} \quad & J_\infty(0) \\ \text{subject to} \quad & \mathbf{K} \in \text{Sparse}(\mathbf{E})\ , \end{aligned} \quad (29)$$

which is a decentralized linear quadratic regulator problem subject to a sparsity constraint on the feedback gain. The sparsity pattern, represented by $\mathbf{E}$, takes the values of $\mathbf{E_\Psi}$ or $\mathbf{E_\Phi}$, depending on the decentralized configuration considered. This problem has already been addressed in [38], for LTI systems. In this paper, the one-step method is employed to obtain an approximate, not necessarily optimal, solution to (29) for an LTI system, as detailed in [38, Section 3.]. However, a numerical solution to the optimization problem (29), such as the one computed by the one-step method, is, generally, not numerically stable. In fact, if the computation of $\mathbf{Q}$ using (27) has any numerical error, arising either from the selection of the columns of the transformation matrix $\mathbf{W}$ or other source that allows for a residual uncontrollable component of $\mathbf{x}(\tau)$ to be summed in (26), then, the cost function is not bounded. In fact, the problem has to be formulated exclusively for the controllable component of the original system, (23), with a feedback control law of the form

$$\mathbf{g}(k) = \bar{\mathbf{g}}(k) - \mathbf{K_1}\mathbf{z_1}(k)\ , \quad (30)$$

where $\mathbf{K_1} \in \mathbb{R}^{S \times S}$ is the feedback gain of the controllable component. Writing (30) in terms of $\mathbf{x}(k)$ and making use of (18), the relation of the feedback gain of the controllable component in relation to the feedback gain of the original system can be written as

$$\mathbf{K} = \mathbf{K_1} \begin{bmatrix} \mathbf{I}_S & \mathbf{0}_{S \times (Z-S)} \end{bmatrix} \mathbf{W}^{-1}\ . \quad (31)$$

The optimization problem (29) is, thus, equivalent to

$$\begin{aligned} \underset{\mathbf{K_1} \in \mathbb{R}^{S \times S}}{\text{minimize}} \quad & J_\infty(0) \\ \text{subject to} \quad & \mathbf{K_1} \begin{bmatrix} \mathbf{I}_S & \mathbf{0}_{S \times (Z-S)} \end{bmatrix} \mathbf{W}^{-1} \in \text{Sparse}(\mathbf{E}) \\ & \mathbf{z_1}(\tau+1) = \mathbf{z_1}(\tau) - \hat{\mathbf{B}}_{\mathbf{g1}}\mathbf{K_1}\mathbf{z_1}(\tau) \\ & \mathbf{z_1}(\tau) = \begin{bmatrix} \mathbf{I}_S & \mathbf{0}_{S \times (Z-S)} \end{bmatrix} \mathbf{W}^{-1}\mathbf{x}(\tau) \\ & \mathbf{z_2}(\tau+1) = \mathbf{z_2}(\tau) \\ & \mathbf{z_2}(\tau) = \begin{bmatrix} \mathbf{0}_{(Z-S) \times S} & \mathbf{I}_{Z-S} \end{bmatrix} \mathbf{W}^{-1}\mathbf{x}(\tau)\ , \tau = 0, 1, \ldots\ , \end{aligned} \quad (32)$$

where $\mathbf{E}$ takes the value of $\mathbf{E_\Psi}$ or $\mathbf{E_\Phi}$, depending on the decentralized configuration considered. A numerical solution to (32) is not unstable. However, it is important to remark that, it is neither of the form of the one-step method optimization problem, nor of other state-of-the-art methods, since the sparsity constraint is not on the gain, but on a linear transformation of the gain. Nevertheless, as evident in the following result, which is adapted from [38, Theorem 1.], the one-step method can be adapted and employed to obtain an approximate solution to (32). The one-step method finds a sub-optimal steady-state gain for the finite-window optimization problem

$$\begin{array}{ll}\underset{\substack{\mathbf{K_1}(\tau)\in\mathbb{R}^{S\times S}\\ \tau=0,\dots,T-1}}{\text{minimize}} & J(0)\\ \text{subject to} & \mathbf{K_1}(\tau)\begin{bmatrix}\mathbf{I}_S & \mathbf{0}_{S\times(Z-S)}\end{bmatrix}\mathbf{W}^{-1}\in\text{Sparse}(\mathbf{E})\\ & \mathbf{z_1}(\tau+1)=\mathbf{z_1}(\tau)-\hat{\mathbf{B}}_{\mathbf{g1}}\mathbf{K_1}\mathbf{z_1}(\tau)\\ & \mathbf{z_1}(\tau)=\begin{bmatrix}\mathbf{I}_S & \mathbf{0}_{S\times(Z-S)}\end{bmatrix}\mathbf{W}^{-1}\mathbf{x}(\tau)\\ & \mathbf{z_2}(\tau+1)=\mathbf{z_2}(\tau)\\ & \mathbf{z_2}(\tau)=\begin{bmatrix}\mathbf{0}_{(Z-S)\times S} & \mathbf{I}_{Z-S}\end{bmatrix}\mathbf{W}^{-1}\mathbf{x}(\tau)\,,\tau=0,\dots,T-1\,,\end{array} \tag{33}$$

which is a relaxation of (32). It takes as solution $\mathbf{K_1}(0)$ as $T\to\infty$, if the limit exits, where $T\in\mathbb{N}$ is the window size, and

$$\begin{aligned}J(k):=&\mathbf{x}^T(T)\mathbf{Q}\mathbf{x}(T)+\sum_{\tau=k}^{T-1}\left(\mathbf{x}^T(\tau)\mathbf{Q}\mathbf{x}(\tau)+(\mathbf{g}(\tau)-\bar{\mathbf{g}}(\tau))^T\mathbf{R}(\mathbf{g}(\tau)-\bar{\mathbf{g}}(\tau))\right)\\ =&\mathbf{z_1}^T(T)\mathbf{Q_1}\mathbf{z_1}(T)+\sum_{\tau=k}^{T-1}\mathbf{z_1}^T(\tau)\mathbf{Q_1}\mathbf{z_1}(\tau)+(\mathbf{g}(\tau)-\bar{\mathbf{g}}(\tau))^T\mathbf{R}(\mathbf{g}(\tau)-\bar{\mathbf{g}}(\tau))\end{aligned}$$

is the finite-window cost function.

Theorem 3.1 (Adapted one-step method)**.** *Let $\mathbf{l}_j$ denote a column vector whose entries are all set to zero except for the j-th one, which is set to 1, and $\boldsymbol{\mathcal{L}}_j:=\operatorname{diag}(\mathbf{l}_j)$. Define a vector $\mathbf{m}_j\in\mathbb{R}^S$ to encode the non-zero entries in the j-th column of $\mathbf{E}$ as*

$$\mathbf{m}_j(i)=\begin{cases}0, & [\mathbf{E}]_{ij}=0\\ 1, & [\mathbf{E}]_{ij}\neq 0\end{cases}\,,\ i=1,...,S\,,$$

and let $\boldsymbol{\mathcal{M}}_j:=\operatorname{diag}(\mathbf{m}_j)$. Then, the gain of the one-step sub-optimal solution to (33) is given by

$$\begin{aligned}&\mathbf{K_1}(\tau)\begin{bmatrix}\mathbf{I}_S\ \mathbf{0}_{S\times(Z-S)}\end{bmatrix}\mathbf{W}^{-1}=\\ &\qquad\sum_{j=1}^{n}(\mathbf{I}-\boldsymbol{\mathcal{M}}_j+\boldsymbol{\mathcal{M}}_j\mathbf{S}(\tau)\boldsymbol{\mathcal{M}}_j)^{-1}\boldsymbol{\mathcal{M}}_j\hat{\mathbf{B}}_{\mathbf{g1}}^T\hat{\mathbf{P}}(\tau+1)\begin{bmatrix}\mathbf{I}_S\ \mathbf{0}_{S\times(Z-S)}\end{bmatrix}\mathbf{W}^{-1}\boldsymbol{\mathcal{L}}_j,\end{aligned} \tag{34}$$

$\tau=0,\dots,T-1$, *where*

$$\mathbf{S}(\tau):=\hat{\mathbf{B}}_{\mathbf{g1}}^T\hat{\mathbf{P}}(\tau+1)\hat{\mathbf{B}}_{\mathbf{g1}}+\mathbf{R}$$

and $\hat{\mathbf{P}}(\tau)$, $\tau = 0, \ldots, T$, *is a symmetric positive semidefinite matrix given by the recurrence*

$$\begin{cases} \hat{\mathbf{P}}(T) = \mathbf{Q_1}(T) & \text{(35a)} \\ \mathbf{P}(\tau+1) = \mathbf{W}^{-T} \begin{bmatrix} \mathbf{I}_S \\ \mathbf{0}_{(Z-S)\times S} \end{bmatrix} \hat{\mathbf{P}}(\tau+1) \begin{bmatrix} \mathbf{I}_S & \mathbf{0}_{S\times(Z-S)} \end{bmatrix} \mathbf{W}^{-1} & \text{(35b)} \\ \mathbf{K}(\tau) = \mathbf{K_1}(\tau) \begin{bmatrix} \mathbf{I}_S & \mathbf{0}_{S\times(Z-S)} \end{bmatrix} \mathbf{W}^{-1} & \text{(35c)} \\ \mathbf{P}(\tau) = \mathbf{Q} + \mathbf{K}^T(\tau)\mathbf{R}\mathbf{K}(\tau) + (\mathbf{A} - \mathbf{B_g}\mathbf{K}(\tau))^T \, \mathbf{P}(\tau+1) \, (\mathbf{A} - \mathbf{B_g}\mathbf{K}(\tau)) & \text{(35d)} \\ \hat{\mathbf{P}}(\tau) = \begin{bmatrix} \mathbf{I}_S & \mathbf{0}_{S\times(Z-S)} \end{bmatrix} \mathbf{W}^T \mathbf{P}(\tau) \mathbf{W} \begin{bmatrix} \mathbf{I}_S \\ \mathbf{0}_{(Z-S)\times S} \end{bmatrix} . & \text{(35e)} \end{cases}$$

Moreover, the one-step sub-optimal solution yields a sub-optimal performance index that follows

$$J^\star(\tau) = \mathbf{x}^T(\tau)\mathbf{P}(\tau)\mathbf{x}(\tau) = \mathbf{z_1}^T(\tau)\hat{\mathbf{P}}(\tau)\mathbf{z_1}(\tau) \, .$$

Proof. See Appendix C. □

Remark 3.1. *The computation of the closed-form solution* (34) *requires* $\mathcal{O}(n^4)$ *floating point operations, using Gaussian elimination. Instead of using it, the exact numeric algorithm proposed in [39] can be, alternatively, applied to* (C.16) *to compute each gain with a computational complexity of* $\mathcal{O}(|\chi|^3)$*, where* $|\chi|$ *denotes the number of nonzero entries of* $\mathbf{E}$*. Usually, in decentralized control applications,* $|\chi| \approx cn$*, where* $c \in \mathbb{N}$ *is a constant, as it is the case for decentralized traffic networks. It, thus, follows that a computational complexity of* $\mathcal{O}(n^3)$ *is achieved, which is identical to the computational complexity of the centralized solution. An efficient MATLAB implementation of this efficient numeric algorithm can be found in the DECENTER toolbox, available at* `https://decenter2021.github.io` *(accessed on 10 July 2021).*

3.1. Summed-up DTUC feedback gain synthesis

Even though the extensive analysis conducted in this section is necessary to gather insight into the problem at hand, as well as to devise numerically stable algorithms to solve it, it can be neatly summarized. First, it was noted that, in general, the traffic dynamics model (12) is not controllable, but the constraint (5) ensures all the components of the system, namely the uncontrollable component, are bounded. Second, a linear feedback control law of the form

$$\mathbf{g}(k) = \bar{\mathbf{g}}(k) - \mathbf{K}\mathbf{x}(k)$$

is sought to regulate the controllable component of (12), where $\bar{\mathbf{g}}(k)$ is based on historic demands on the network $\mathbf{d}_{\text{hist}}(k)$ and given by (24). Third, the state-of-the-art decentralized methods of synthesizing $\mathbf{K}$ are not numerically stable for this formulation of the problem. Thus, the one-step method, put forward in [38, Section 3.], was adapted, as detailed in Theorem 3.1, which provides a numerically stable algorithm. The iterative procedure of the one-step method is detailed in Table 3. Note that, for the computation of both $\bar{\mathbf{g}}(k)$ and $\mathbf{K}$, matrices $\mathbf{W}$ and $\hat{\mathbf{B}}_{\mathbf{g1}}$ must be computed beforehand, according to (18) and (19), decomposing the LTI system (12) according to the Canonical Structure Theorem. Furthermore, the gain $\mathbf{K}$ can be computed offline.

Table 3: Augmented one-step algorithm for the computation of a steady-state feedback gain.

1. **Initialization:**
   (a) Select a large enough finite-window length T
   (b) $\hat{\mathbf{P}}(T) = \mathbf{Q_1}$
   (c) $\tau = T - 1$
2. **Do:**
   (a) Compute $\mathbf{K}(\tau)$ making use of (34) and (35c)
   (b) Compute $\mathbf{P}(\tau+1)$ making use of (35b)
   (c) Compute $\mathbf{P}(\tau)$ making use of (35d)
   (d) Compute $\hat{\mathbf{P}}(\tau)$ making use of (35e)
   (e) $\tau = \tau - 1$

   While: $\tau \leq 0$
3. **Return:** $\mathbf{K}(0)$

3.2. Post-processing

It is, now, important to incorporate the constraints (1) and (2) into the DTUC strategy. Having that in mind, for each cycle k, the computational unit of each junction j, has to adjust the solution provided by the linear quadratic optimization problem, $g_s(k)$, $s \in \mathcal{F}_j$, according to (1) and (2). As proposed in [8, 32], the introduction of these constraints amounts to solving

$$\begin{aligned} \underset{\tilde{g}_s(k),\, s\in\mathcal{F}_j}{\text{minimize}} \quad & \frac{1}{2}\sum_{s\in F_f} \left(\tilde{g}_s(k) - g_s(k)\right)^2 \\ \text{subject to} \quad & \tilde{g}_s(k) \geq g_{s,min}\ , s \in \mathcal{F}_j \\ & \sum_{s\in\mathcal{F}_j} \tilde{g}_s(k) + L_j = C\ . \end{aligned} \tag{36}$$

Note that, the optimization problems (36) for $j \in \{1, \ldots, J\}$, that each computational unit $\mathcal{T}_j$ has to solve, are independent and rely, exclusively, on data known to $\mathcal{T}_j$. Thus, they can be solved in parallel, by each computational unit $\mathcal{T}_j$, in a distributed manner, without requiring additional communication. Define

$\tilde{\mathbf{g}}_\mathbf{j} := \mathrm{col}(\tilde{g}_s(k) - g_{s,\min}, s \in \mathcal{F}_j)$, where the discrete time instant k was dropped for lighter notation. Expanding the objective function of the optimization above and rewriting the constraints yields

$$\begin{aligned} \underset{\tilde{\mathbf{g}}_\mathbf{j} \in \mathbb{R}^{|\mathcal{F}_j|}}{\text{minimize}} \quad & \frac{1}{2} \tilde{\mathbf{g}}_\mathbf{j}^T \mathrm{diag}(\mathbf{d}) \tilde{\mathbf{g}}_\mathbf{j} - \mathbf{a}^T \tilde{\mathbf{g}}_\mathbf{j} \\ \text{subject to} \quad & \mathbf{0} \leq \tilde{\mathbf{g}}_\mathbf{j} \leq \mathbf{b} \\ & \mathbf{1}^T \tilde{\mathbf{g}}_\mathbf{j} = c \ , \end{aligned} \tag{37}$$

where $\mathbf{d} = \mathbf{1}_{|\mathcal{F}_j|}$, $\mathbf{a} = \mathrm{col}\left(g_s(k) - g_{s,\min}, s \in \mathcal{F}_j\right)$, and

$$c = C - L_j - \sum_{s \in \mathcal{F}_j} g_{s,\min}(k) \ .$$

Since there is no upper bound on $\tilde{\mathbf{g}}_\mathbf{j}$, $\mathbf{b}$ can be set to $\mathbf{b} = c\mathbf{1}_{|f_j|}$, for instance, which does not modify the solution of the original optimization problem (36). Not only is optimization problem (37) convex, but it is also a quadratic continuous knapsack problem, whose solution can be found making use of very efficient algorithms. Note that (37) is of the same form as the problem solved in [40]. In fact, the optimal solution to (37) can be solved using the iterative algorithm presented in [40, Section 3.] in $|\mathcal{F}_j|$ iterations or less.

4. Decentralized Decoupled Traffic-responsive Urban Control (D2TUC)

In this section, another decentralized traffic-responsive signal control strategy is presented, which is inspired in the QPC approach, proposed in [32, Section 4.2.] for a centralized configuration, as an attempt to improve the performance of TUC. The linear-quadratic method explored in the previous section relies on a cost function that does not allow to weight the state as one would ideally want. In fact, the weighting matrix $\mathbf{Q}$ in (26) must have a particular structure, given by (27), instead of ideally being set to $\mathbf{Q} = \mathrm{diag}(1/x_{1,\max}, \ldots, 1/x_{Z,\max})$. Having this limitation in mind, one can, alternatively, compute the green times of each link independently, *i.e.*

$$\mathbf{G}(k) = \bar{\mathbf{G}}(k) - \mathbf{K}\mathbf{x}(k) \ , \tag{38}$$

where $\mathbf{K} \in \mathbb{R}^{Z \times Z}$ is the gain matrix of this approach, which is synthesized based on the LTI system (10), and $\bar{\mathbf{G}}(k)$ is a feedforward term computed using an historical demand, as defined in the sequel. Note that, similarly to DTUC, the gain $\mathbf{K}$ can be computed offline. First, as detailed in the following result, the LTI system (10) of a feasible traffic network, as defined in Definition 2.2, is controllable.

Proposition 4.1. Consider a feasible traffic network characterized by $(\mathcal{G}, \mathbf{T}, \mathbf{t_0})$. Then, the store-and-forward LTI system (10) is controllable.

Proof. See Appendix D. □

Next, one assumes that an historical demand $\mathbf{d}_{\text{hist}}(k)$ is available. Rewrite (10) as

$$\mathbf{x}(k+1) = \mathbf{x}(k) + \mathbf{B_G}(\mathbf{G}(k) - \bar{\mathbf{G}}(k)) + C\boldsymbol{\epsilon}(k)\ , \tag{39}$$

where $\boldsymbol{\epsilon}(k)$ is considered to be a disturbance, given by $\boldsymbol{\epsilon}(k) := \mathbf{d}_{\text{hist}}(k) + \mathbf{B_G}\bar{\mathbf{G}}(k)$. In order to apply a decentralized regulator to (39), $\bar{\mathbf{G}}(k)$ is selected such that the disturbance $\boldsymbol{\epsilon}(k)$ is minimal, *i.e.*, $\bar{\mathbf{G}}(k)$ is given by the solution to

$$\underset{\bar{\mathbf{G}}(k)\in\mathbb{R}^S}{\text{minimize}} \quad \|\boldsymbol{\epsilon}(k)\|^2 \quad ,$$

for $k \in \mathbb{N}_0$. The optimization problem above is a least squares optimization problem, whose solution is

$$\bar{\mathbf{G}}(k) = -\left(\mathbf{B_G}^T\mathbf{B_G}\right)^{-1}\mathbf{B_G}^T\mathbf{d}_{\text{hist}}(k)$$

if $\mathbf{B_G} \in \mathbb{R}^{Z\times Z}$ is full rank, which is an immediate consequence of Proposition 4.1.

Since (39) is controllable, it is possible to write the quadratic cost function as

$$J_\infty(k) = \sum_{\tau=k}^{\infty} \mathbf{x}(\tau)^T\mathbf{Q}\mathbf{x}(\tau) + (\mathbf{G}(k) - \bar{\mathbf{G}}(k))^T\mathbf{R}(\mathbf{G}(k) - \bar{\mathbf{G}}(k))\ , \tag{40}$$

where $\mathbf{Q} \succeq \mathbf{0}$ and $\mathbf{R} \succ \mathbf{0}$ are selected matrices of appropriate dimensions. Note that, contrarily to (26), the state weighting matrix $\mathbf{Q}$ can be selected freely, as long as it is positive semidefinite. Thus, it can be set to the ideal $\mathbf{Q} = \text{diag}(1/x_{1,\max}, \ldots, 1/x_{Z,\max})$, to penalize the relative occupancy of each link. Note that the fact that the green time of each link can be selected independently allows for more flexibility and would, evidently, lead to better performance if it could be applied. Nevertheless, the green times of each link are subject to the green times of the stages in which they are given r.o.w.. For that reason, this approach requires additional post-processing, not only to split the green times of the links among the stages, but also to impose the constraints (1) and (2), whereas the post-processing step of the DTUC strategy has only to enforce the latter.

Furthermore, note that, due to the limitation on the communication links between junctions in a decentralized configuration, as put forward in Section 2.4, there are constraints on the structure of the feedback gain $\mathbf{K}$ of the control law (38). Consider junction j. The command action of a stage $s \in \mathcal{F}_j$ is computed making use of information know to the computational unit $\mathcal{T}_j$, exclusively. The set of links whose queue length is available to computational unit $\mathcal{T}_j$ is: i) Ψ_j, as defined in (16), for configuration Ψ; and ii) Φ_j, as defined in (17), for configuration Φ. Thus, for configuration Ψ, $G_z(k)$ is of the form

$$G_z(k) = [\bar{\mathbf{G}}(k)]_z - \sum_{e_i\in\Psi_j} [K]_{zi}x_i(k)\ ,$$

and, for configuration Φ, $G_z(k)$ is of the form

$$G_z(k) = [\bar{\mathbf{G}}(k)]_z - \sum_{e_i\in\Phi_j} [K]_{zi}x_i(k)\ \ .$$

As a matter of fact, it is equivalent to imposing a sparsity constraint $\mathbf{K} \in \mathrm{Sparse}(\mathbf{E}_{\mathbf{\Psi}})$, where $\mathbf{E}_{\mathbf{\Psi}} \in \mathbb{R}^{Z\times Z}$ is such that

$$\forall j \in \{1,\ldots,J\}\ \forall e_z \in \mathcal{E}_j^-\ \forall w \in \{1,\ldots,Z\}\ (e_w \in \Psi_j \implies [\mathbf{E}_{\mathbf{\Psi}}]_{zw} \neq 0) \wedge (e_w \notin \Psi_j \implies [\mathbf{E}_{\mathbf{\Psi}}]_{zw} = 0)\ , \quad (41)$$

for the decentralized configuration Ψ and $\mathbf{K} \in \mathrm{Sparse}(\mathbf{E}_{\mathbf{\Phi}})$ for configuration Φ, where $\mathbf{E}_{\mathbf{\Phi}} \in \mathbb{R}^{Z\times Z}$ is defined in the same manner as (41) replacing Ψ_j with Φ_j.

Thus, the linear quadratic optimization problem becomes

$$\begin{aligned} &\underset{\mathbf{K}\in\mathbb{R}^{Z\times Z}}{\text{minimize}} && J_\infty(0) \\ &\text{subject to} && \mathbf{K} \in \mathrm{Sparse}(\mathbf{E})\ , \end{aligned} \quad (42)$$

which is a decentralized linear quadratic regulator problem subject to a sparsity constraint on the feedback gain. The sparsity pattern, represented by $\mathbf{E}$, takes the values of $\mathbf{E}_{\mathbf{\Psi}}$ or $\mathbf{E}_{\mathbf{\Phi}}$, depending on the decentralized configuration that is considered. This problem has already been addressed in [38] for LTI systems. In this paper, the one-step method is employed, to obtain an approximate, not necessarily optimal, solution to (42) for an LTI system, as detailed in [38, Section 3].

4.1. Post-processing

It is, now, necessary to incorporate the constraints (1), (2), and allocate the green time of each link among the available stages. Having that in mind, for each cycle k, the computational unit of each junction j, has to adjust the solution of the linear quadratic optimization problem, $G_z(k), z \in \{1,\ldots,Z\}$, according to $\mathbf{G}(k) = \mathbf{S}\mathbf{g}(k)$, (1), and (2). It seems, at first sight, that the best option is to split the green times of the links among the stages and imposing the constraints (1) and (2) simultaneously. However, given that the allocation of the stage times is what influences most significantly the performance of the regulator, it is performed beforehand and constraints (1) and (2) are enforced posteriorly.

First, the optimal stage times $g_s(k), s \in \{1,\ldots,S\}$ are obtained solving

$$\underset{\mathbf{g}(k)\in\mathbb{R}^S}{\text{minimize}} \quad \|\mathbf{G}(k) - \mathbf{S}\mathbf{g}(k)\|^2\ , \quad (43)$$

where $\mathbf{g}(k) = \mathrm{col}(g_s(k), s \in \{1,\ldots,S\})$, which is a standard least squares optimization problem. However, (43) is not written in a form to allow for the distributed computation across the computational units of each junction. For that reason, consider, without loss of generality, the numbering convention proposed in Section 2.1. For a minimum complete stage strategy, one can write $\mathbf{S} = \mathrm{diag}(\mathbf{S_1},\ldots,\mathbf{S_J})$, where $\mathbf{S_j} \in \mathbb{R}^{|\mathcal{F}_j|\times\nu_i^-}$. Thus, the decentralized optimization problem

$$\underset{\mathbf{g_j}(k)\in\mathbb{R}^S}{\text{minimize}} \quad \|\mathbf{G_j}(k) - \mathbf{S_j}\mathbf{g_j}(k)\|^2\ , \quad (44)$$

where $\mathbf{g_j}(k) := \mathrm{col}(g_s(k), s \in \mathcal{F}_j)$ and $\mathbf{G_j} := \mathrm{col}(G_z(k), e_z \in \mathcal{E}_j^-)$, for $j = 1, \dots, J$, is equivalent to (43). The optimization problem (44) is also a least squares problem, whose solution is given by

$$\mathbf{g_j}(k) = (\mathbf{S_j}^T\mathbf{S_j})^{-1}\mathbf{S_j}^T\mathbf{G}(k) \;, \tag{45}$$

if $\mathbf{S_j}$ is full rank, which is required by the condition 4 of Definition 2.3 of a minimum complete stage strategy. Second, the constraints (1) and (2) are posteriorly imposed, using the same procedure as described in Section 3.2, to determine the D2TUC stage green times for each junction $\tilde{\mathbf{g}}_\mathbf{j}$.

5. Numeric simulation

As a means of assessing the performance of the decentralized control strategies proposed in this paper, they are applied to a simulated urban traffic network of the city center of Chania, Greece, whose model was kindly provided by the authors of [32]. The performance of DTUC and D2TUC decentralized methods for both decentralized configurations are compared between themselves, with the centralized solution provided by TUC [11], and the centralized equivalent of D2TUC. The numerical simulations are carried out considering the nonlinear model (15), put forward in Section 2.2, which offers a realistic macroscopic simulation of a real traffic network.

The Chania urban traffic network, whose topology graph is depicted in Fig. 3, consists of $J = 16$ signalized junctions, and $L = 60$ links. The cycle time is set to $C = 90$ s, the simulation sampling time to $T = 5$ s, and the parameter that adjusts the sensibility of upstream gating to $c_{ug} = 0.85$. This network is feasible and a minimum complete stage strategy was used, whose details are omitted. The command action weighting matrix is set to $\mathbf{R} = 10^{-4}\mathbf{I}$, for both DTUC and D2TUC strategies, which was adjusted using a trial-and-error procedure [32]. The performance of the strategies simulated in this section was found to exhibit very little sensibility to the choice of the weighting matrix $\mathbf{R}$.

Two objective functions, proposed in [32, Section 5.2], are used to assess the performance of the proposed decentralized approaches: i) the total time spent (TTS)

$$\mathrm{TTS} = T\sum_k \sum_{z=1}^{Z} x_z(k)$$

and ii) the relative queue balance (RQB)

$$\mathrm{RQB} = \sum_k \sum_{z=1}^{Z} \frac{x_z^2(k)}{x_{z,max}} \;.$$

Similarly to [32], these criteria are applied to the average of the values of $x_z(k_T)$ over each cycle interval C.

The simulations were carried out for one scenario of high and another of intermediate demand. The simulation was run for 10 control cycles, corresponding to 15 minutes. The initial link queues were randomly

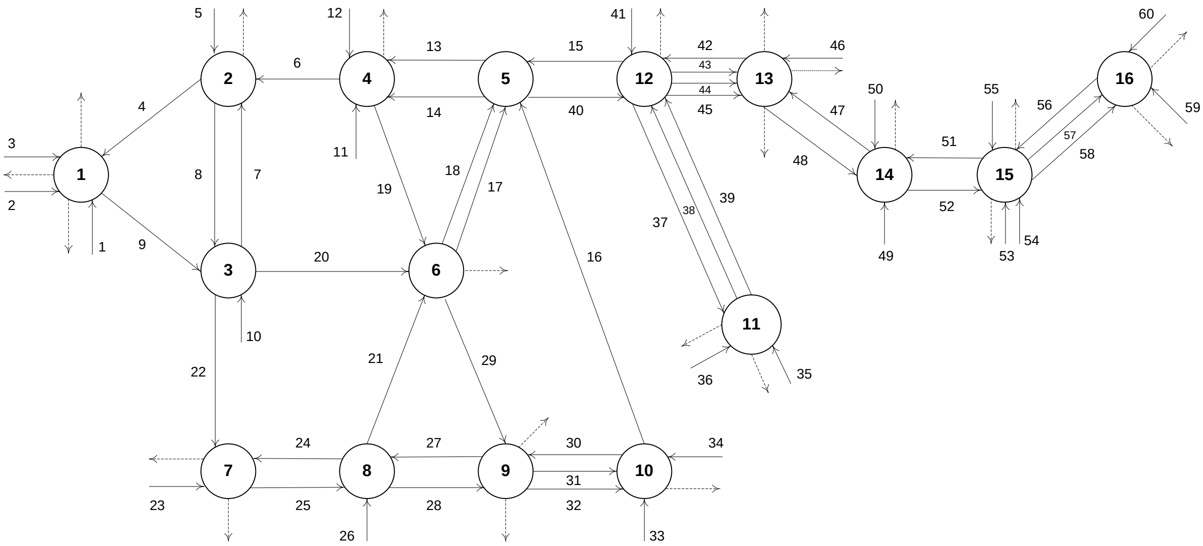

Figure 3: Chania urban traffic network topology graph, kindly provided by the authors of [32].

generated, as well as the historic demand $\mathbf{d}_{\text{hist}}(k)$, which was held constant during the simulations. Both parameters were kept unchanged among all the simulations carried out. The results of the performance criteria are presented in Table 4, for the high demand scenario, and in Table 5, for the intermediate demand scenario. Figs. 4 and 5 depict the evolution of the sum of the absolute value of the entries of the controllable and uncontrollable components, for the high and intermediate demand scenarios, respectively. Fig. 6 shows the evolution of illustrative link occupancy and stage time, related to junction 12, for the D2TUC strategy with decentralized configuration Φ.

Table 4: Performance criteria of simulation for the high demand scenario, and comparison of the performance of the decentralized solutions with the corresponding centralized solutions.

Strategy	TUC	DTUC Ψ	DTUC Φ	D2TUC Cent.	D2TUC Ψ	D2TUC Φ
RQB	1512	2155	1581	1438	1577	1494
	–	+42.5%	+4.57%	–	+9.67%	+3.88%
TTS	84.25	100.9	85.95	86.10	86.59	84.16
	–	+19.7%	+2.02%	–	+0.573%	-2.24%

First, it is visible in Figs. 4 and 5 that both decentralized methods, for both decentralized configurations, and for both demand scenarios, successfully stabilize the traffic dynamics, regulating the controllable component of the link occupancy. It is interesting to note that, despite the fact that the demand is constant throughout each simulation, the uncontrollable component actually decreases with time, which is a consequence of the use of simulation nonlinear effects, such as (5) and upstream gating, as described in

Table 5: Performance criteria of simulation for the intermediate demand scenario, and comparison of the performance of the decentralized solutions with the corresponding centralized solutions.

Strategy	TUC	DTUC Ψ	DTUC Φ	D2TUC Cent.	D2TUC Ψ	D2TUC Φ
RQB	527.6	937.9	670.0	469.4	731.8	514.8
	–	+77.8%	+27.0%	–	+55.9%	+9.67%
TTS	39.82	53.16	44.15	38.67	45.86	38.76
	–	+33.5%	+10.9%	–	+18.6%	+0.246%

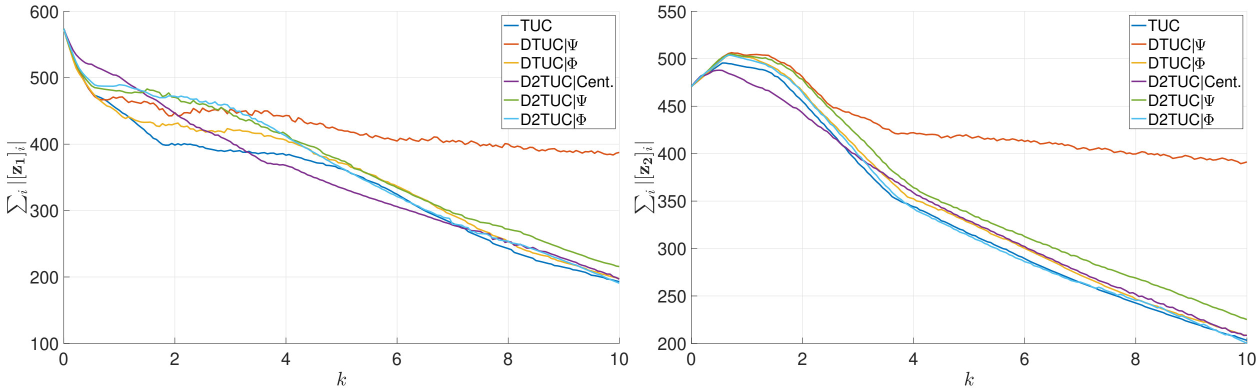

(a) Controllable.

(b) Uncontrollable.

Figure 4: Evolution of the sum of the absolute value of the state components for the high demand scenario.

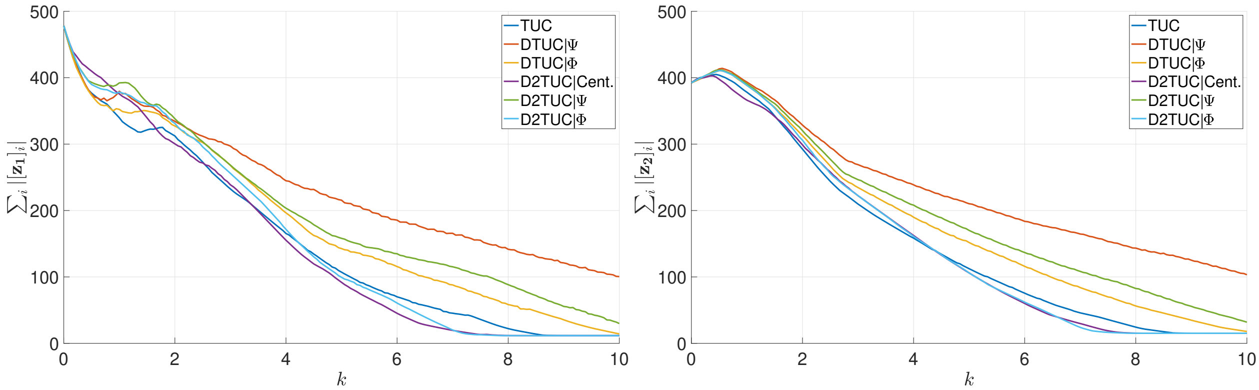

(a) Controllable.

(b) Uncontrollable.

Figure 5: Evolution of the sum of the absolute value of the state components for the high demand scenario.

Section 2.2. Second, recall that the DTUC and D2TUC methods, proposed herein, are inspired in the TUC approach and QPC method, presented, respectively in [11] and [32], whose performance is compared in [32]. Similarly to that comparison, Tables 4 and 5 show that it is possible to improve the performance of TUC making use of the centralized D2TUC method. Third, as an example, in Fig. 6 the effect of up-

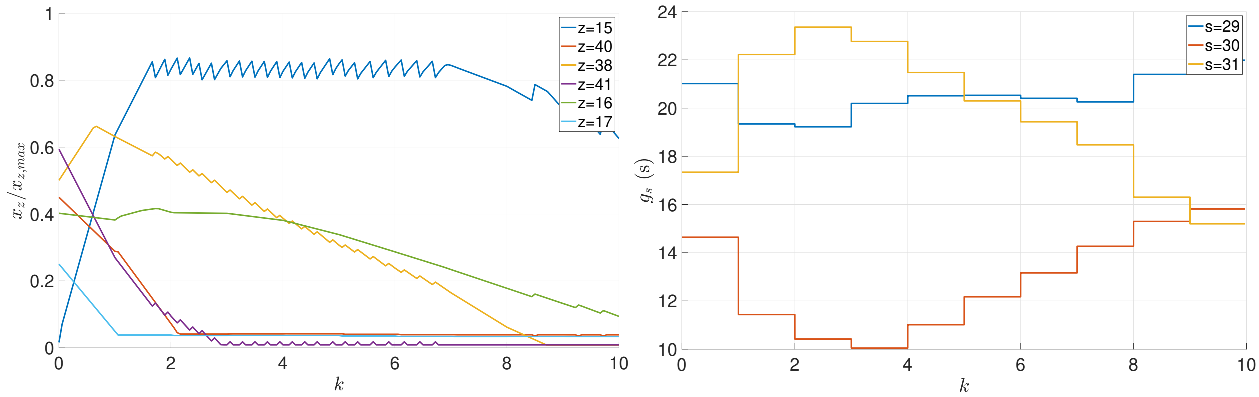

(a) Link occupancy of links related to junction 12.

(b) Stage green times of junction 12.

Figure 6: Evolution of illustrative link occupancy and stage green time for the D2TUC strategy with decentralized configuration Φ.

Table 6: Performance comparison between the decentralized solution of D2TUC with configuration Φ and TUC.

Demand scenario	Intermediate		High	
Strategy	TUC	D2TUC Φ	TUC	D2TUC Φ
RQB	527.6	514.8	1512	1494
	–	-2.43%	–	-1.19%
TTS	39.82	38.76	84.25	84.16
	–	-2.73%	–	-0.11%

stream gating throughout the simulation is noticeable, preventing link 15 from overloading, due to the high demand. Furthermore, the decentralized solution is shown to successfully reduce congestion. Fourth, recall that, contrarily to the DTUC method, the D2TUC method allows to design the regulator with the weighting ratios necessary to balance the relative occupancy of the links. In fact, the results presented in Tables 4 and 5 show that there is a significant reduction on the RQB of the D2TUC method compared with the DTUC method, for both the centralized and decentralized solutions and for both demand scenarios. Fifth, it is important to remark that due to the very limited link load information when computing the green times of the stages at a junction, it is expected that the performance of decentralized solutions is generally poorer. However, although in a decentralized configuration it is particularly hard to achieve a balanced relative occupancy of the links, due to the heavy communication limitations, the D2TUC decentralized solution, using the decentralized configuration Φ, leads to an increase of only 3.88% and 9.67% of the RQB in relation to the best centralized solution, for the high and intermediate demand scenarios, respectively. Sixth, despite the heavy communication restrictions, the TTS of the D2TUC decentralized solution, using the decentralized configuration Φ, is identical to the performance of the best centralized solution, resulting in an increase of 2.24% and decrease of 0.246%, for the high and intermediate demand scenarios, respectively. This result indicates that, as far as the ability to reduce congestion is concerned, the performance of the best decentralized and centralized method are similar. On top of that, the infrastructure required by the application of the centralized solution is significantly greater than the necessary for the application of the decentralized solution. Note that the increase in performance of the decentralized solution was obtained by chance, and is only possible due to the use of the nonlinear simulation model, which does not correspond to the controller synthesis model. Seventh, it is important to remark that the decentralized solution of the D2TUC method, with the decentralized configuration Φ, is able to consistently match the performance of TUC, for both demand scenarios, as it is possible to notice analyzing Table 6. Eighth, there is a significant performance improvement by using the decentralized configuration Φ rather than Ψ. Recall, from Section 2.4, that the decentralized configuration Ψ requires no communication between junctions regarding the decentralized controller, whereas the decentralized configuration Φ takes advantage of the communication links required by a decentralized observer to receive link occupancy information known to neighboring junctions. In this particular example, only 21 bidirectional communication links are required to apply the decentralized configuration Φ, which are the same necessary for the implementation of a decentralized observer.

In this section, both decentralized methods presented in this paper for the signal control problem in large-scale congested urban roads were validated, yielding very promising results. In fact, making use of only 21 bidirectional communication links between junctions of the traffic network, it was possible to consistently match the performance of TUC. The implementation of a decentralized solution requires significantly less infrastructure, and as the computation of the green times can be performed in a distributed manner across the computational units of each junction and very efficiently, cheap microcontrollers are suitable for the computational units. The significant reduction of the implementation cost of signal control for large-scale traffic networks allows for the implementation of such strategies on networks whose centralized solution is not feasible.

6. Conclusion

Signal control strategies designed in a centralized framework require many communication links, serious processing power, and infrastructure for the centralized coordination. As a result, strategies based on a centralized framework are not easily scalable. The use of decentralized signal control solutions for large-scale urban traffic networks is a solution to this problem, since it allows for the implementation of such strategies on networks whose centralized implementation is challenging and expensive due to the dimension of the network. However, very little work has been carried out regarding the design of decentralized signal control solutions for large-scale urban traffic networks. In this paper, two decentralized traffic-responsive signal control methods, designated as DTUC and D2TUC, based on different formulations of the store-and-forward model, are derived and their performance is assessed. Sufficient conditions for the controllability of the considered store-and-forward models are also presented. Both methods are devised as the solution to a decentralized linear quadratic regulator problem, which results in a very efficient computation of the green times for each stage. It is considered that each intersection is associated with one computational unit, with limited computational power and memory, which controls the traffic signals of the incoming links. The proposed methods are validated resorting to numerical simulations of the urban traffic network of Chania, Greece, and their performance is compared with the performance obtained with TUC, a state-of-the-art centralized solution which has already been applied experimentally in three cities in Europe. The simulations are carried out for two different demand scenarios and for two different decentralized configurations. First, it is shown that both methods successfully stabilize the traffic dynamics, regulating the link occupancy. Second, the D2TUC decentralized method is shown to match the performance of TUC, for both demand scenarios considered, as far as the balance of the relative link occupancy and vehicle throughput are concerned. Third, the computations required by both methods are very efficient and performed in a distributed framework, requiring only cheap microcontrollers as computational units. For these reasons, the solution proposed in this paper is very compelling. Not only is it suitable for the implementation to large-scale traffic networks, with a fraction of the cost that would be required for a centralized implementation, but it also matches the performance of a state-of-the-art centralized approach.

Acknowledgements

This work was supported by the Fundação para a Ciência e a Tecnologia (FCT) through LARSyS - FCT Project UIDB/50009/2020 and through the FCT project DECENTER [LISBOA-01-0145-FEDER-029605], funded by the Programa Operacional Regional de Lisboa 2020 and PIDDAC programs. The authors thank Dr. Konstantinos Aboudolas, Dr. Elias Kosmatopoulos, and Dr. Markos Papageorgiou for their kindness in providing the Chania urban road model and for an early discussion on the controllability of the model.

Appendix A. Derivation of LTI traffic network dynamics for the store-and-forward model

The detailed derivation of the three expressions for the store-and-forward model of a traffic network (6),(10), and (12), is detailed in this section. As a means of lightening the notation, Einstein summation convention is used. Rewriting (3) as

$$\mathbf{x}(k+1)^i = \mathbf{x}(k)^i + C\mathbf{q}(k)^i - C\mathbf{u}(k)^i - C\mathbf{s}(k)^i + C\mathbf{d}(k)^i \ ,$$

where $\mathbf{q}(k) := \mathrm{col}(q_1(k), ..., q_Z(k)) \in \mathbb{R}^Z$ and $\mathbf{s}(k) := \mathrm{col}(s_1(k), ..., s_Z(k)) \in \mathbb{R}^Z$, (4) as

$$\mathbf{q}(k)^i = \mathbf{T}^i_j \mathbf{u}(k)^j \ ,$$

and $\mathbf{s}(k)^i = t_{i,0}\mathbf{q}(k)^i$ as

$$\mathbf{s}(k)^i = t_{i,0}\boldsymbol{\delta}^i_j\mathbf{q}(k)^j \ ,$$

where $\boldsymbol{\delta}^i_j$ denotes the Kronecker delta, one arrives at

$$\begin{aligned}\mathbf{x}(k+1)^i &= \boldsymbol{\delta}^i_j\mathbf{x}(k)^j + C(\boldsymbol{\delta}^i_k - t_{i,0}\boldsymbol{\delta}^i_k)\mathbf{q}(k)^k - C\boldsymbol{\delta}^i_j\mathbf{u}(k)^j + C\mathbf{d}(k)^i \\ &= \boldsymbol{\delta}^i_j\mathbf{x}(k)^j + C\left((\boldsymbol{\delta}^i_k - t_{i,0}\boldsymbol{\delta}^i_k)\mathbf{T}^k_j - \boldsymbol{\delta}^i_j\right)\mathbf{u}(k)^j + C\mathbf{d}(k)^i \\ &= \mathbf{A}^i_j\mathbf{x}(k)^j + {\mathbf{B_u}}^i_j\mathbf{u}(k)^j + C\mathbf{d}(k)^i \ ,\end{aligned} \tag{A.1}$$

with

$$\mathbf{A}^i_j = \boldsymbol{\delta}^i_j \quad \text{and} \quad {\mathbf{B_u}}^i_j = C\left((\boldsymbol{\delta}^i_k - t_{i,0}\boldsymbol{\delta}^i_k)\mathbf{T}^k_j - \boldsymbol{\delta}^i_j\right) \ , \tag{A.2}$$

which is of the same form as (6). Writing (A.2) in matrix notation yields $\mathbf{A} = \mathbf{I}_Z$ and (7). Rewriting (8) as

$$\mathbf{u}(k)^l = \frac{S_l}{C}\boldsymbol{\delta}^l_j\mathbf{G}(k)^j \ ,$$

(A.1) can be rewritten as

$$\begin{aligned}\mathbf{x}(k+1)^i &= \boldsymbol{\delta}^i_j\mathbf{x}(k)^j + \left((\boldsymbol{\delta}^i_k - t_{i,0}\boldsymbol{\delta}^i_k)\mathbf{T}^k_l - \boldsymbol{\delta}^i_l\right)S_l\boldsymbol{\delta}^l_j\mathbf{G}(k)^j + C\mathbf{d}(k)^i \\ &= \mathbf{A}^i_j\mathbf{x}(k)^j + {\mathbf{B_G}}^i_j\mathbf{u}(k)^j + C\mathbf{d}(k)^i \ ,\end{aligned}$$

with

$${\mathbf{B_G}}^i_j = C\left((\boldsymbol{\delta}^i_k - t_{i,0}\boldsymbol{\delta}^i_k)\mathbf{T}^k_l - \boldsymbol{\delta}^i_l\right)S_l\boldsymbol{\delta}^l_j \ , \tag{A.3}$$

which is of the same form as (10). Writing (A.3) in matrix notation yields (11). Rewriting (9) as

$$\mathbf{G}(k)^m = \mathbf{S}^m_j\mathbf{g}(k)^j \ ,$$

(A.1) can be rewritten as

$$\begin{aligned}\mathbf{x}(k+1)^i &= \boldsymbol{\delta}^i_j\mathbf{x}(k)^j + \left((\boldsymbol{\delta}^i_k - t_{i,0}\boldsymbol{\delta}^i_k)\mathbf{T}^k_l - \boldsymbol{\delta}^i_l\right)S_l\boldsymbol{\delta}^l_m\mathbf{S}^m_j\mathbf{g}(k)^j + C\mathbf{d}(k)^i \\ &= \mathbf{A}^i_j\mathbf{x}(k)^j + {\mathbf{B_g}}^i_j\mathbf{u}(k)^j + C\mathbf{d}(k)^i \ ,\end{aligned}$$

with

$${\mathbf{B_g}}^i_j = C\left((\boldsymbol{\delta}^i_k - t_{i,0}\boldsymbol{\delta}^i_k)\mathbf{T}^k_l - \boldsymbol{\delta}^i_l\right)S_l\boldsymbol{\delta}^l_m\mathbf{S}^m_j \ , \tag{A.4}$$

which is of the same form as (12). Writing (A.4) in matrix notation yields (13).

Appendix B. Proof of Proposition 3.1

Consider a feasible traffic network characterized by $(\mathcal{G}, \mathbf{T}, \mathbf{t_0})$ and a minimum complete stage strategy characterized by stage matrix $\mathbf{S}$. Let $\boldsymbol{\mathcal{C}}$ be the controllability matrix of the store-and-forward LTI system (12), which is given by

$$\boldsymbol{\mathcal{C}} = \begin{bmatrix}\mathbf{B_g} & \mathbf{AB_g} & \dots & \mathbf{A}^{Z-1}\mathbf{B_g}\end{bmatrix} \ .$$

Given that $\mathbf{A} = \mathbf{I}_Z$, it is evident that $\boldsymbol{\mathcal{C}} \in \mathbb{R}^{Z\times ZS}$ has $\text{rank}(\boldsymbol{\mathcal{C}}) = \text{rank}(\mathbf{B_g})$. Furthermore, by (13) and Sylvester rank inequality [41, Theorem 8.1.2], one has

$$\text{rank}(\mathbf{B_g}) \geq \text{rank}(\mathbf{S}) + \text{rank}(\mathbf{B_G}) - Z\,. \tag{B.1}$$

In Appendix D, it is proved that, for a feasible traffic network characterized by $(\mathcal{G}, \mathbf{T}, \mathbf{t_0})$, then $\text{rank}(\mathbf{B_G}) = Z$. Furthermore, considering, without loss of generality, the numbering convention proposed in Section 2.1, for a minimum complete stage strategy, the stage matrix $\mathbf{S}$ can be written as $\mathbf{S} = \text{diag}(\mathbf{S_1}, \ldots, \mathbf{S_J})$, where $\mathbf{S_j} \in \mathbb{R}^{|\mathcal{F}_j|\times \nu_i^-}$. Given that condition 4 of the Definition 2.3 requires each matrix $\mathbf{S_j}$, $j \in \{1, \ldots, J\}$, to be full rank, and the rank of a block diagonal matrix is equal to the sum of the rank of the block matrices, then $\mathbf{S}$ is full rank. Additionally, for a minimum complete stage strategy, $S \leq Z$, thus $\text{rank}(\mathbf{S}) = S$. For this reason, from (B.1), one has $\text{rank}(\mathbf{B_g}) \geq S$. In addition, since $\mathbf{B_g} \in \mathbb{R}^{Z\times S}$, then $\text{rank}(\mathbf{B_g}) \leq \min(Z, S) = S$. Therefore, $\text{rank}(\boldsymbol{\mathcal{C}}) = \text{rank}(\mathbf{B_g}) = S \leq Z$.

Appendix C. Derivation of the augmented one-step method

The proposed derivation of the augmented one-step method for the computation of decentralized LQR gains, which correspond to a sub-optimal solution to the finite-window decentralized LQR problem, follows the Lagrange-multiplier approach detailed, for instance, in [42]. The goal of using this approach is to ease the inclusion of the sparsity constraint $\mathbf{K}(\tau) \in \text{Sparse}(\mathbf{E})$, the state equation, and the linear feedback action, which allows to write (33) as an unconstrained optimization problem.

Writing an augmented performance index, $J'(0)$, that takes into account a linear feedback action, as well as the state equation, yields

$$\begin{aligned}
J'(0) =& \mathbf{x}^T(T)\mathbf{Q}\mathbf{x}(T) + \sum_{\tau=0}^{T-1} \mathbf{x}^T(\tau)\left(\mathbf{Q} + \mathbf{K}^T(\tau)\mathbf{R}\mathbf{K}(\tau)\right)\mathbf{x}(\tau) \\
&+ \sum_{\tau=0}^{T-1} \boldsymbol{\lambda}^T(\tau+1)\left[(\mathbf{A} - \mathbf{B_g}\mathbf{K}(\tau))\,\mathbf{x}(\tau) - \mathbf{x}(\tau+1)\right] \\
=& \mathbf{z_1}^T(T)\mathbf{Q_1}\mathbf{z_1}(T) + \sum_{\tau=0}^{T-1} \mathbf{z_1}^T(\tau)\left(\mathbf{Q_1} + \mathbf{K_1}^T(\tau)\mathbf{R}\mathbf{K_1}(\tau)\right)\mathbf{z_1}(\tau) \\
&+ \sum_{\tau=0}^{T-1} \boldsymbol{\lambda_1}^T(\tau+1)\left[\left(\mathbf{I}_S - \hat{\mathbf{B}}_{\mathbf{g1}}\mathbf{K_1}(\tau)\right)\mathbf{z_1}(\tau) - \mathbf{z_1}(\tau+1)\right]\,,
\end{aligned} \tag{C.1}$$

where $\boldsymbol{\lambda}(\tau+1) \in \mathbb{R}^n$ and $\boldsymbol{\lambda_1}(\tau+1) \in \mathbb{R}^S$ are the Lagrange-multipliers associated with each of the constraints that arise from the state equations. The augmented performance index (C.1) is often written, for convenience, as a function of the Hamiltonian, defined, in this case, as

$$H(\tau) := \mathbf{x}^T(\tau)\left(\mathbf{Q} + \mathbf{K}^T(\tau)\mathbf{R}\mathbf{K}(\tau)\right)\mathbf{x}(\tau) + \boldsymbol{\lambda}^T(\tau+1)\left(\mathbf{A} - \mathbf{B_g}\mathbf{K}(\tau)\right)\mathbf{x}(\tau)$$

for the whole system, and as

$$H_1(\tau) := \mathbf{z_1}^T(\tau)\left(\mathbf{Q_1} + \mathbf{K_1}^T(\tau)\mathbf{R}\mathbf{K_1}(\tau)\right)\mathbf{z_1}(\tau) + \boldsymbol{\lambda_1}^T(\tau+1)\left(\mathbf{I}_S - \hat{\mathbf{B}}_{\mathbf{g1}}\mathbf{K_1}(\tau)\right)\mathbf{z_1}(\tau)\,,$$

for the controllable component of the state, which yields

$$\begin{aligned} J'(0) &= \mathbf{x}^T(T)\mathbf{Q}\mathbf{x}(T) - \boldsymbol{\lambda}^T(T)\mathbf{x}(T) + H(0) + \sum_{\tau=1}^{T-1}\left(H(\tau) - \boldsymbol{\lambda}^T(\tau)\mathbf{x}(\tau)\right) \\ &= \mathbf{z_1}^T(T)\mathbf{Q_1}\mathbf{z_1}(T) - \boldsymbol{\lambda_1}^T(T)\mathbf{z_1}(T) + H_1(0) + \sum_{\tau=1}^{T-1}\left(H_1(\tau) - \boldsymbol{\lambda_1}^T(\tau)\mathbf{z_1}(\tau)\right)\,. \end{aligned} \tag{C.2}$$

Taking the differential of the augmented performance index (C.2), one obtains

$$\begin{aligned} dJ'(0) &= (2\mathbf{Q}\mathbf{x}(T) - \boldsymbol{\lambda}(T))^T d\mathbf{x}(T) \\ &+ \left(\frac{\partial H(0)}{\partial \mathbf{x}(0)}\right)^T d\mathbf{x}(0) + \sum_{\tau=1}^{T}\left(\frac{\partial H(\tau-1)}{\partial \boldsymbol{\lambda}(\tau)} - \mathbf{x}(\tau)\right)^T d\boldsymbol{\lambda}(\tau) + \left(\frac{\partial H(0)}{\partial \mathrm{vec}\,(\mathbf{K}(0))}\right)^T \mathrm{dvec}\,(\mathbf{K}(0)) \\ &+ \sum_{\tau=1}^{T-1}\left[\left(\frac{\partial H(\tau)}{\partial \mathrm{vec}\,(\mathbf{K}(\tau))}\right)^T \mathrm{dvec}\,(\mathbf{K}(\tau)) + \left(\frac{\partial H(\tau)}{\partial \mathbf{x}(\tau)} - \boldsymbol{\lambda}(\tau)\right)^T d\mathbf{x}(\tau)\right]\,, \end{aligned} \tag{C.3}$$

for the whole system, and

$$\begin{aligned} dJ'(0) &= (2\mathbf{Q_1}\mathbf{z_1}(T) - \boldsymbol{\lambda_1}(T))^T d\mathbf{z_1}(T) \\ &+ \left(\frac{\partial H_1(0)}{\partial \mathbf{z_1}(0)}\right)^T d\mathbf{z_1}(0) + \sum_{\tau=1}^{T}\left(\frac{\partial H_1(\tau-1)}{\partial \boldsymbol{\lambda_1}(\tau)} - \mathbf{z_1}(\tau)\right)^T d\boldsymbol{\lambda_1}(\tau) + \left(\frac{\partial H_1(0)}{\partial \mathrm{vec}\,(\mathbf{K_1}(0))}\right)^T \mathrm{dvec}\,(\mathbf{K_1}(0)) \\ &+ \sum_{\tau=1}^{T-1}\left[\left(\frac{\partial H_1(\tau)}{\partial \mathrm{vec}\,(\mathbf{K_1}(\tau))}\right)^T \mathrm{dvec}\,(\mathbf{K_1}(\tau)) + \left(\frac{\partial H_1(\tau)}{\partial \mathbf{z_1}(\tau)} - \boldsymbol{\lambda_1}(\tau)\right)^T d\mathbf{z_1}(\tau)\right]\,, \end{aligned} \tag{C.4}$$

for the controllable component of the state.

Define the set χ of integer pairs of the form (i,j) to index the non-zero entries of $\mathbf{E}$ as

$$\begin{cases} (i,j) \in \chi & \text{if } [\mathbf{E}]_{ij} \neq 0 \\ (i,j) \notin \chi & \text{otherwise} \end{cases}, i = 1,...,m,\ j = 1,...,n\,. \tag{C.5}$$

The necessary conditions for the constrained minimum follow from (C.3) and from the sparsity constraint. Note that, although it is straightforward to introduce the sparsity constraint using (C.3), the same is not true for (C.4). For a fixed initial state $\mathbf{x}(0)$ and free final state $\mathbf{x}(T)$, the constrained minimum requires that $dJ'(0) = 0$ holds for any: i) $d\mathbf{x}(\tau)$, with $\tau = 1,...,T$; ii) $d\boldsymbol{\lambda}(\tau)$, with $\tau = 1,...,T$; and iii) $\mathbf{l}_i^T d\mathbf{K}(\tau)\mathbf{l}_j$, with $\tau = 0,...,T-1$ and $(i,j) \in \chi$. Hence, it follows that

$$\mathbf{x}(\tau+1) = \frac{\partial H(\tau)}{\partial \boldsymbol{\lambda}(\tau+1)},\ \tau = 0,...,T-1\,, \tag{C.6a}$$

$$\boldsymbol{\lambda}(\tau) = \frac{\partial H(\tau)}{\partial \mathbf{x}(\tau)},\ \tau = 1,...,T-1\,, \tag{C.6b}$$

$$\mathbf{l}_i^T \frac{\partial H(\tau)}{\partial \mathbf{K}(\tau)} \mathbf{l}_j = 0 \ , \tau = 0, ..., T-1, \ (i,j) \in \chi \ , \tag{C.6c}$$

$$\mathbf{l}_i^T \mathbf{K}(\tau) \mathbf{l}_j = 0 \ , \tau = 0, ..., T-1, \ (i,j) \notin \chi \ , \tag{C.6d}$$

and

$$\boldsymbol{\lambda}(T) = 2\mathbf{Q}(T)\mathbf{x}(T) \ , \tag{C.6e}$$

where $\mathbf{l}_i$ is defined as in Theorem 3.1. Above, (C.6a) is the state equation, (C.6b) is the costate equation, (C.6c) is the stationary condition, (C.6d) is the sparsity constraint, and (C.6e) is the boundary condition. It is interesting to remark the usefulness of the Hamiltonian function, which allows to write the constraints of the optimization problem as neat identities involving its partial derivatives. As the form of the boundary condition suggests, the Lagrage-multipliers can possibly be written as $\boldsymbol{\lambda}(\tau) = 2\mathbf{P}(\tau)\mathbf{x}(\tau)$, where $\mathbf{P}(\tau)$ is a symmetric positive semidefinite matrix. In that case, from the boundary condition (C.6e), it follows that $\mathbf{P}(T) = \mathbf{Q}$. In fact, making use of the costate equation (C.6b), this hypothesis yields

$$\mathbf{P}(\tau)\mathbf{x}(\tau) = \left(\mathbf{Q} + \mathbf{K}^T(\tau)\mathbf{R}\mathbf{K}(\tau)\right)\mathbf{x}(\tau) + \left(\mathbf{A} - \mathbf{B_g}\mathbf{K}(\tau)\right)^T \mathbf{P}(\tau+1)\mathbf{x}(\tau+1) \ ,$$

$\tau = 0, \dots, T-1$, which holds for every $\mathbf{x}(\tau)$ if and only if

$$\mathbf{P}(\tau) = \mathbf{Q} + \mathbf{K}^T(\tau)\mathbf{R}(\tau)\mathbf{K}(\tau) + \left(\mathbf{A} - \mathbf{B_g}\mathbf{K}(\tau)\right)^T \mathbf{P}(\tau+1)\left(\mathbf{A} - \mathbf{B_g}\mathbf{K}(\tau)\right) \ . \tag{C.7}$$

For this reason, the hypothesis on the form of the Lagrange multipliers, $\boldsymbol{\lambda}(k) = 2\mathbf{P}(k)\mathbf{x}(k)$, is valid, and $\mathbf{P}(k)$ is given by the recursive closed-form expression (C.7). Note, however, that this recurrence is sensible to numerical error. One can also prove, by induction, that

$$J(\tau) = \mathbf{x}^T(\tau)\mathbf{P}(\tau)\mathbf{x}(\tau) \ , \tag{C.8}$$

for $\tau = 0, \dots, T$. First, note that $J(T) = \mathbf{x}^T(T)\mathbf{P}(T)\mathbf{x}(T)$, which follows directly from the definition of the finite-horizon performance index (3) and the fact that $\mathbf{P}(T) = \mathbf{Q}$. Moreover, for $\tau = 0, \dots, T-1$, it follows from (3) and the linear command action that

$$J(\tau) = J(\tau+1) + \mathbf{x}^T(\tau)\left(\mathbf{Q} + \mathbf{K}^T(\tau)\mathbf{R}\mathbf{K}(\tau)\right)\mathbf{x}(\tau) \ . \tag{C.9}$$

Substituting the inductive hypothesis (C.8) in (C.9) and making use of the closed-loop system dynamics yields

$$J(\tau) = \mathbf{x}^T(\tau)\left(\mathbf{Q} + \mathbf{K}^T(\tau)\mathbf{R}\mathbf{K}(\tau) + \left(\mathbf{A} - \mathbf{B_g}\mathbf{K}(\tau)\right)^T \mathbf{P}(\tau+1)\left(\mathbf{A} - \mathbf{B_g}\mathbf{K}(\tau)\right)\right)\mathbf{x}(\tau) \ ,$$

which by comparison with (C.7) concludes the proof by induction. Carrying out the same analysis for the controllable component of the system, it is possible to arrive at the corresponding identities. That is, the

Lagrage-multipliers of the controllable component can be written as $\boldsymbol{\lambda_1}(\tau) = 2\hat{\mathbf{P}}(\tau)\mathbf{z_1}(\tau)$, where $\hat{\mathbf{P}}(\tau)$ is a symmetric positive semidefinite matrix, which allows to write

$$\hat{\mathbf{P}}(\tau) = \mathbf{Q_1} + \mathbf{K_1}^T(\tau)\mathbf{R}\mathbf{K_1}(\tau) + \left(\mathbf{I}_S - \hat{\mathbf{B}}_{\mathbf{g1}}\mathbf{K_1}(\tau)\right)^T \hat{\mathbf{P}}(\tau+1)\left(\mathbf{I}_S - \hat{\mathbf{B}}_{\mathbf{g1}}\mathbf{K_1}(\tau)\right) , \tag{C.10}$$

with boundary condition

$$\hat{\mathbf{P}}(T) = \mathbf{Q_1} .$$

Also, it follows that

$$J(\tau) = \mathbf{z_1}^T(\tau)\hat{\mathbf{P}}(\tau)\mathbf{z_1}(\tau) . \tag{C.11}$$

Equaling (C.11) and (C.8), and using the transformation (18), one obtains

$$\mathbf{P}(\tau) = \mathbf{W}^{-T}\begin{bmatrix}\mathbf{I}_S \\ \mathbf{0}_{(Z-S)\times S}\end{bmatrix}\hat{\mathbf{P}}(\tau)\begin{bmatrix}\mathbf{I}_S & \mathbf{0}_{S\times(Z-S)}\end{bmatrix}\mathbf{W}^{-1} , \tag{C.12}$$

which can be manipulated to yield

$$\mathbf{W}^T\mathbf{P}(\tau)\mathbf{W} = \begin{bmatrix}\hat{\mathbf{P}}(\tau) & \mathbf{0}_{r\times(Z-S)} \\ \mathbf{0}_{(Z-S)\times r} & \mathbf{0}_{(Z-S)\times(Z-S)}\end{bmatrix} .$$

Transformation (C.12) can be inverted yielding

$$\hat{\mathbf{P}}(\tau) = \begin{bmatrix}\mathbf{I}_S & \mathbf{0}_{S\times(Z-S)}\end{bmatrix}\mathbf{W}^T\mathbf{P}(\tau)\mathbf{W}\begin{bmatrix}\mathbf{I}_S \\ \mathbf{0}_{(Z-S)\times S}\end{bmatrix} . \tag{C.13}$$

Making use of (C.6c), and using, also, the closed-loop system dynamics of the whole system, one can write

$$\mathbf{l}_i^T\left[\mathbf{R}\mathbf{K}(\tau)\mathbf{x}(\tau)\mathbf{x}^T(\tau) - \mathbf{B_g}^T\mathbf{P}(\tau+1)\left(\mathbf{A} - \mathbf{B_g}\mathbf{K}(\tau)\right)\mathbf{x}(\tau)\mathbf{x}^T(\tau)\right]\mathbf{l}_j = 0 , \tag{C.14}$$

for all $(i,j) \in \chi$ and $\tau = 0, \dots T-1$. Note that (C.14) depends on $\mathbf{x}(\tau), \tau = 0, \dots T-1$, which is not readily available in a decentralized formulation. For that reason, unlike the centralized finite-horizon problem, finding all the solutions to (C.14), being the global minimum among them, is not possible without the knowledge of $\mathbf{x}(\tau), \tau = 0, \dots T-1$. For that reason, it is only possible to compute one sub-optimal solution using this equation, designated herein by the one-step solution. Introducing the sparsity constraint (C.6d), this solution satisfies

$$\begin{cases}\mathbf{l}_i^T\left[\mathbf{S}(\tau)\mathbf{K}(\tau) - \mathbf{B_g}^T\mathbf{P}(\tau+1)\mathbf{A}\right]\mathbf{l}_j = 0 & , \ (i,j) \in \chi \\ \mathbf{l}_i^T\mathbf{K}(\tau)\mathbf{l}_j = 0 & , \ (i,j) \notin \chi\end{cases} , \ \tau = 0, \dots, T-1, \tag{C.15}$$

where

$$\mathbf{S}(\tau) := \mathbf{R} + \mathbf{B_g}^T\mathbf{P}(\tau+1)\mathbf{B_g} .$$

Substituting (31) and (C.13) in (C.15), yields

$$\begin{cases} \mathbf{l}_i^T \left[\left(\mathbf{S}(\tau)\mathbf{K_1}(\tau) - \hat{\mathbf{B}}_{\mathbf{g1}}^T \hat{\mathbf{P}}(\tau+1) \right) \begin{bmatrix} \mathbf{I}_S & \mathbf{0}_{S\times(Z-S)} \end{bmatrix} \mathbf{W}^{-1} \right] \mathbf{l}_j = 0 & , \ (i,j) \in \chi \\ \mathbf{l}_i^T \mathbf{K}(\tau) \mathbf{l}_j = 0 & , \ (i,j) \notin \chi \end{cases} , \ \tau = 0, \ldots, T-1, \tag{C.16}$$

where $\mathbf{S}(\tau)$ can be written as

$$\mathbf{S}(\tau) := \mathbf{R} + \hat{\mathbf{B}}_{\mathbf{g1}}^T \hat{\mathbf{P}}(\tau+1) \hat{\mathbf{B}}_{\mathbf{g1}} \, .$$

Note that (C.16) has the same form as the equation that arises in the LTI formulation of the one-step method for the decentralized estimation problem, put forward in [43, Theorem 4.1]. From [43, Appendix A.], the sub-optimal gain is, then, given by (34). Note that it is not possible to determine $\mathbf{K}_1(\tau)$ explicitly from the solution obtained for the gain, given by (34). For that reason it is not possible to compute the propagation of $\hat{\mathbf{P}}(\tau)$ in (C.10). To circumvent this issue one may propagate $\mathbf{P}(\tau)$ instead, which makes use of $\mathbf{K}(\tau)$, which is easily computed using (34). Then, $\hat{\mathbf{P}}(\tau)$ is obtained with transformation (C.13). One has, now, a set of equations that allows for the backpropagation of $\hat{\mathbf{P}}(\tau)$ and $\mathbf{K_1}(\tau)$. In short, perform the following iteration for $\tau = T-1, \ldots, 0$: i) compute $\mathbf{K}(\tau)$, making use of $\hat{\mathbf{P}}(\tau+1)$; ii) compute $\mathbf{P}(\tau+1)$, using transformation (C.12) and $\hat{\mathbf{P}}(\tau+1)$; iii) backpropagate $\mathbf{P}(\tau)$, using (C.7), $\mathbf{K}(\tau)$, and $\mathbf{P}(\tau+1)$; and iv) compute $\hat{\mathbf{P}}(\tau)$, using transformation (C.13) and $\mathbf{P}(\tau)$.

Appendix D. Proof of proposition 4.1

Consider a feasible traffic network characterized by $(\mathcal{G}, \mathbf{T}, \mathbf{t_0})$, as given by Definition 2.2. Consider a directed walk of length p, $p_{\mathcal{G}}(p) = \{e_1, \ldots, e_{p-1}\}$, whose sequence of vertices is $(v_1, v_2 \ldots, v_p)$. The probability of a vehicle traveling from v_2 to v_p by following $p_{\mathcal{G}}(p)$ is denoted by $P(p_{\mathcal{G}}(p))$. Let $\mathcal{P}_{i,j}^p$ denote the set of walks of length p between edges e_i and e_j. Then,

$$\forall i,j \in \{1, \ldots, \tilde{Z}\} \; \forall p_{\mathcal{G}}(p) \in \mathcal{P}_{i,j}^p \;\; \lim_{p\to\infty} P(p_{\mathcal{G}}(p)) = 0 \, , \tag{D.1}$$

which is proved by contradiction. Note that (D.1) is, by the definition of limit, equivalent to

$$\forall i,j \in \{1, \ldots, \tilde{Z}\} \; \forall p_{\mathcal{G}}(p) \in \mathcal{P}_{i,j}^p \; \forall \epsilon > 0 \;\; \exists \bar{p} \in \mathbb{N} : p > \bar{p} \implies P(p_{\mathcal{G}}(p)) < \epsilon \, . \tag{D.2}$$

Assume, by contradiction, that (D.2) is false, *i.e.*, there exists $i,j \in \{1, \ldots, \tilde{Z}\}$, $p_{\mathcal{G}}(p) \in \mathcal{P}_{i,j}^p$, and $\epsilon > 0$, such that, for all $\bar{p} \in \mathbb{N}$, there exists $p > \bar{p}$, such that $P(p_{\mathcal{G}}(p)) \geq \epsilon$. Thus, there exists $i,j \in \{1, \ldots, \tilde{Z}\}$, $p_{\mathcal{G}}(p) \in \mathcal{P}_{i,j}^p$, $\epsilon > 0$, $\bar{p}$ arbitrarily large, and $p > \bar{p}$ such that $P(p_{\mathcal{G}}(p)) \geq \epsilon$. Given that there exists an arbitrarily large p and the traffic network is finite, which is a requirement for a feasible traffic network, then there exists a nonempty set of edges $\mathcal{E}$ which appear in the walk $p_{\mathcal{G}}(p)$ an arbitrarily large number of times. Thus, if there is an edge $e \in \mathcal{E}$ that appears in the walk $p_{\mathcal{G}}(p)$ an arbitrarily large number of times, then there exists a sub-walk starting and ending at the same edge $e \in \mathcal{E}$, which appears in the walk $p_{\mathcal{G}}$ an arbitrarily large number of times. Thus, the probability of progressing from edge e via such sub-walk back to edge e is unitary, otherwise, as p grows arbitrarily large, eventually $P(p_{\mathcal{G}}(p)) < \epsilon$. Therefore, if there is a walk that starts and returns with unitary probability back to the starting edge, the network cannot be open, which is a contradiction, thus proving (D.1). Furthermore, consider matrix $\tilde{\mathbf{T}} := (\mathbf{I} - \mathrm{diag}(\mathbf{t_0}))\mathbf{T}$. Note that $[\tilde{\mathbf{T}}]_{i,j}$ represents the probability of turning from link j to link i and not exiting the network in link i. Thus, $[\tilde{\mathbf{T}}^2]_{i,j}$ is the probability of a vehicle traveling from link j to link i, via one and only one link, without exiting the network, neither in the intermediate link, nor in link i. It is then possible to write

$$[\tilde{\mathbf{T}}^n]_{i,j} = \sum_{k_1} \cdots \sum_{k_{n-1}} [\tilde{\mathbf{T}}]_{i,k_1} \cdots [\tilde{\mathbf{T}}]_{k_{n-2},k_{n-1}} [\tilde{\mathbf{T}}]_{k_{n-1},j} = \sum_{p_{\mathcal{G}} \in \mathcal{P}_{j,i}^{n+2}} P(p_{\mathcal{G}}(p)) \, .$$

Thus, making use of (D.1), one has

$$\lim_{n \to \infty} \tilde{\mathbf{T}}^n = \mathbf{0} \, . \tag{D.3}$$

According to [44, Lemma 1.1], (D.3) is equivalent to the spectral radius of $\tilde{\mathbf{T}}$, denoted by $\rho(\tilde{\mathbf{T}})$, satisfying $\rho(\tilde{\mathbf{T}}) < 1$. Therefore, as the absolute value of the eigenvalues of a matrix are bounded by its spectral radius, $\lambda = 1$ cannot be an eigenvalue of $\tilde{\mathbf{T}}$. Thus, $(\tilde{\mathbf{T}} - \mathbf{I})\mathbf{x} = 0$ for $\mathbf{x} \in \mathbb{R}$ implies $\mathbf{x} = \mathbf{0}$, which is equivalent to $(\tilde{\mathbf{T}} - \mathbf{I})$ being invertible, *i.e.*,

$$\mathrm{rank}((\mathbf{I} - \mathrm{diag}(\mathbf{t_0}))\mathbf{T} - \mathbf{I}) = Z \, .$$

Finally, the LTI system (12) is, by definition, controllable if and only if the controllability matrix

$$\boldsymbol{\mathcal{C}} := \begin{bmatrix} \mathbf{B_G} & \mathbf{A}\mathbf{B_G} & \dots & \mathbf{A}^{Z-1}\mathbf{B_G} \end{bmatrix}$$

is full rank. Since $\mathbf{A} = \mathbf{I}_Z$, then $\mathrm{rank}(\boldsymbol{\mathcal{C}}) = \mathrm{rank}(\mathbf{B_G})$. Thus, by (11) and the Sylvester rank inequality [41, Theorem 8.1.2], one has

$$\mathrm{rank}(\mathbf{B_G}) \geq \mathrm{rank}((\mathbf{I} - \mathrm{diag}(\mathbf{t_0}))\mathbf{T} - \mathbf{I}) + \mathrm{rank}(\mathrm{diag}(S_1, \dots, S_Z)) - Z = Z \, .$$

Since $\mathbf{B_G} \in \mathbb{R}^{Z \times Z}$ and $\mathrm{rank}(\mathbf{B_G}) = Z$, it follows that the controllability matrix is full rank, thus completing the proof.

References

[1] H. R. TO, M. M. Barker, White paper european transport policy for 2010: time to decide, Commission of the European Communities Brussels, 2001.

[2] A. Sims, K. Dobinson, Scat the sydney coordinated adaptive traffic system: philosophy and benefits, in: International Symposium on Traffic Control Systems, 1979, Berkeley, California, USA, Vol. 2, 1979.

[3] P. Hunt, D. Robertson, R. Bretherton, R. Winton, Scoot-a traffic responsive method of coordinating signals, Tech. rep. (1981).

[4] J.-J. Henry, J. L. Farges, J. Tuffal, The prodyn real time traffic algorithm, in: Control in Transportation Systems, Elsevier, 1984, pp. 305–310.

[5] V. Mauro, C. Di Taranto, Utopia, IFAC Proceedings Volumes 23 (2) (1990) 245–252.

[6] P. Mirchandani, L. Head, A real-time traffic signal control system: architecture, algorithms, and analysis, Transportation Research Part C: Emerging Technologies 9 (6) (2001) 415–432.

[7] M. Papageorgiou, C. Diakaki, V. Dinopoulou, A. Kotsialos, Y. Wang, Review of road traffic control strategies, Proceedings of the IEEE 91 (12) (2003) 2043–2067.

[8] C. Diakaki, Integrated control of traffic flow in corridor networks, Ph.D. thesis, Department of Production Engineering and Management, Technical University of Crete (1999).

[9] D. C. Gazis, R. B. Potts, The oversaturated intersection, Tech. rep. (1963).

[10] V. Dinopoulou, C. Diakaki, M. Papageorgiou, Simulation investigations of the traffic-responsive urban control strategy tuc, in: 2000 International IEEE Conference on Intelligent Transportation Systems, IEEE, 2000, pp. 458–463.

[11] C. Diakaki, M. Papageorgiou, K. Aboudolas, A multivariable regulator approach to traffic-responsive network-wide signal control, Control Engineering Practice 10 (2) (2002) 183–195.

[12] C. Diakaki, V. Dinopoulou, K. Aboudolas, M. Papageorgiou, E. Ben-Shabat, E. Seider, A. Leibov, Extensions and new applications of the traffic-responsive urban control strategy: Coordinated signal control for urban networks, Transportation Research Record 1856 (1) (2003) 202–211.

[13] C. Diakaki, M. Papageorgiou, T. McLean, Application and evaluation of the integrated traffic-responsive urban corridor control strategy in-tuc in glasgow, in: Proceedings of the 78th Annual Meeting of the Transportation Research Board, 1999.

[14] V. Dinopoulou, C. Diakaki, M. Papageorgiou, Application and evaluation of the signal traffic control strategy tuc in chania, Journal of Intelligent Transportation Systems 9 (3) (2005) 133–143.

[15] E. Smaragdis, V. Dinopoulou, K. Aboudolas, C. Diakaki, M. Papageorgiou, Application of the extended traffic signal control strategy tuc to the southampton urban road network, IFAC Proceedings Volumes 36 (14) (2003) 31–36.

[16] S. Bereg, J. M. Díaz-Báñez, M. A. Lopez, T. Rozario, K. Valavanis, A decentralized geometric approach for the formation keeping in unmanned aircraft navigation, in: 2015 International Conference on Unmanned Aircraft Systems (ICUAS), 2015, pp. 989–997.

[17] R. T. Thien, Y. Kim, Decentralized formation flight via pid and integral sliding mode control, Aerospace Science and Technology 81 (2018) 322–332.

[18] D. Viegas, P. Batista, P. Oliveira, C. Silvestre, Decentralized observers for position and velocity estimation in vehicle formations with fixed topologies, Systems & Control Letters 61 (3) (2012) 443–453. doi:10.1016/j.sysconle.2011.12.004.

[19] C. Yuan, S. Licht, H. He, Formation learning control of multiple autonomous underwater vehicles with heterogeneous nonlinear uncertain dynamics, IEEE Transactions on Cybernetics (99) (2017) 1–15.

[20] D. Ivanov, U. Monakhova, M. Ovchinnikov, Nanosatellites swarm deployment using decentralized differential drag-based control with communicational constraints, Acta Astronautica 159 (2019) 646–657.

[21] I. Prodan, L. Lefevre, D. Genon-Catalot, et al., Distributed model predictive control of irrigation systems using cooperative controllers, IFAC-PapersOnLine 50 (1) (2017) 6564–6569.

[22] X.-F. Xie, S. F. Smith, L. Lu, G. J. Barlow, Schedule-driven intersection control, Transportation Research Part C: Emerging Technologies 24 (2012) 168–189.

[23] P. Varaiya, Max pressure control of a network of signalized intersections, Transportation Research Part C: Emerging Technologies 36 (2013) 177–195.

[24] T. Le, P. Kovács, N. Walton, H. L. Vu, L. L. Andrew, S. S. Hoogendoorn, Decentralized signal control for urban road networks, Transportation Research Part C: Emerging Technologies 58 (2015) 431–450.

[25] S. El-Tantawy, B. Abdulhai, An agent-based learning towards decentralized and coordinated traffic signal control, in: 13th International IEEE Conference on Intelligent Transportation Systems, IEEE, 2010, pp. 665–670.

[26] D. Manolis, T. Pappa, C. Diakaki, I. Papamichail, M. Papageorgiou, Centralised versus decentralised signal control of large-scale urban road networks in real time: a simulation study, IET Intelligent Transport Systems 12 (8) (2018) 891–900.

[27] A. H. Chow, R. Sha, S. Li, Centralised and decentralised signal timing optimisation approaches for network traffic control, Transportation Research Part C: Emerging Technologies 113 (2020) 108–123. doi:https://doi.org/10.1016/j.trc.2019.05.007.

[28] A. H. F. Chow, R. Sha, Y. Li, Adaptive control strategies for urban network traffic via a decentralized approach with user-optimal routing, IEEE Transactions on Intelligent Transportation Systems 21 (4) (2020) 1697–1704. doi:10.1109/TITS.2019.2955425.

[29] Z. Su, A. H. Chow, R. Zhong, Adaptive network traffic control with an integrated model-based and data-driven approach and a decentralised solution method, Transportation Research Part C: Emerging Technologies 128 (2021) 103154. doi:https://doi.org/10.1016/j.trc.2021.103154.

[30] G. Befekadu, I. Erlich, Robust decentralized controller design for power systems using matrix inequalities approaches, in: 2006 IEEE Power Engineering Society General Meeting, 2006, pp. 8 pp.–. doi:10.1109/PES.2006.1709077.

[31] F. Blanchini, E. Franco, G. Giordano, Structured-lmi conditions for stabilizing network-decentralized control, in: 52nd IEEE Conference on Decision and Control, 2013, pp. 6880–6885. doi:10.1109/CDC.2013.6760979.

[32] K. Aboudolas, M. Papageorgiou, E. Kosmatopoulos, Store-and-forward based methods for the signal control problem in large-scale congested urban road networks, Transportation Research Part C: Emerging Technologies 17 (2) (2009) 163–174.

[33] D. B. West, et al., Introduction to graph theory, Vol. 2, Prentice hall Upper Saddle River, NJ, 1996.

[34] W. D. Wallis, A beginner's guide to graph theory, Springer Science & Business Media, 2010.

[35] G. Padmavathi, D. Shanmugapriya, M. Kalaivani, et al., A study on vehicle detection and tracking using wireless sensor networks, Wireless Sensor Network 2 (02) (2010) 173.

[36] Q. Wang, J. Zheng, H. Xu, B. Xu, R. Chen, Roadside magnetic sensor system for vehicle detection in urban environments, IEEE Transactions on Intelligent Transportation Systems 19 (5) (2017) 1365–1374.

[37] W. J. Rugh, Linear system theory, Prentice-Hall, Inc., 1996.

[38] D. Viegas, P. Batista, P. Oliveira, C. Silvestre, Distributed controller design and performance optimization for discrete-time linear systems, Optimal Control Applications and Methods (2020) 1–18doi:10.1002/oca.2669.

[39] L. Pedroso, P. Batista, Efficient algorithm for the computation of the solution to a sparse matrix equation in distributed control theory, Mathematics 9 (13) (2021) 1497. doi:10.3390/math9131497.

[40] R. Helgason, J. Kennington, H. Lall, A polynomially bounded algorithm for a singly constrained quadratic program, Mathematical Programming 18 (1) (1980) 338–343.

[41] V. V. Prasolov, Problems and theorems in linear algebra, Vol. 134, American Mathematical Soc., 1994.

[42] F. L. Lewis, D. Vrabie, V. L. Syrmos, Optimal control, John Wiley & Sons, 2012.

[43] D. Viegas, P. Batista, P. Oliveira, C. Silvestre, Discrete-time distributed kalman filter design for formations of autonomous vehicles, Control Engineering Practice 75 (2018) 55–68.

[44] J. Theys, et al., Joint Spectral Radius: theory and approximations, Ph. D. dissertation, 2005.